Single-channel study of the spasmodic mutation α1A52S in recombinant rat glycine receptors

Andrew J. R. Plested, Paul J. Groot-Kormelink, David Colquhoun and Lucia G. Sivilotti

Department of Pharmacology, University College London, Gower Street, London WC1E 6BT, UK

Inherited defects in glycine receptors lead to hyperekplexia, or startle disease. A mutant mouse, *spasmodic*, that has a startle phenotype, has a point mutation (A52S) in the glycine receptor α1 subunit. This mutation reduces the sensitivity of the receptor to glycine, but the mechanism by which this occurs is not known. We investigated the properties of A52S recombinant receptors by cell-attached patch-clamp recording of single-channel currents elicited by 30–10000 μM glycine. We used heteromeric receptors, which resemble those found at adult inhibitory synapses. Activation mechanisms were fitted directly to single channel data using the HJCFIT method, which includes an exact correction for missed events. In common with wild-type receptors, only mechanisms with three binding sites and extra shut states could describe the observations. The most physically plausible of these, the 'flip' mechanism, suggests that preopening isomerization to the flipped conformation that follows binding is less favoured in mutant than in wild-type receptors, and, especially, that the flipped conformation has a 100-fold lower affinity for glycine than in wild-type receptors. In contrast, the efficacy of the gating reaction was similar to that of wild-type heteromeric receptors. The reduction in affinity for the flipped conformation accounts for the reduction in apparent cooperativity seen in the mutant receptor (without having to postulate interaction between the binding sites) and it accounts for the increased EC_{50} for responses to glycine that is seen in mutant receptors. This mechanism also predicts accurately the faster decay of synaptic currents that is observed in *spasmodic* mice.

(Received 18 December 2006; accepted after revision 21 February 2007; first published online 1 March 2007)
Corresponding author Lucia G Sivilotti: Department of Pharmacology, University College London, Gower Street, London WC1E 6BT, UK. Email: l.sivilotti@ucl.ac.uk

Ligand-gated ion channels mediate fast signalling between nerve and muscle and between neurones in the brain and in the spinal cord. The nicotinic receptor superfamily includes receptors for acetylcholine, GABA, serotonin and glycine. Inhibitory glycine receptors in the brainstem and spinal cord control muscle tone and locomotion. Those found at adult inhibitory synapses are probably heteropentamers formed of α1 and β subunits (Lynch, 2004).

Mutations that damage the expression, membrane incorporation or native function of the glycine receptor result in human congenital 'startle disease' or hyperekplexia. Major hyperekplexia is a rare, mostly autosomal dominant human disease (OMIM no. 149400) that is often misdiagnosed as epilepsy, manifests itself by an excessive startle response to mild sensory stimuli and leads to uncontrolled falls. In neonates, excessive startle is associated with generalized stiffness, myoclonic attacks and apnoea (Bakker *et al.* 2006). Treatment with clonazepam is usually effective (Praveen *et al.* 2001). Many human and murine hyperekplexia mutations have been identified (Lynch, 2004), but there is little correspondence between the apparent severity of the mutation and the phenotype. The most interesting naturally occurring mutations (from the point of view of receptor mechanisms) are those that alter, but do not abolish the function of the glycine receptor, such as the alanine to serine mutation at position 52 in the α1 subunit (α1 A52S) that is responsible for the recessive hyperekplexia phenotype of the mutant mouse *spasmodic (spd)* (Lane *et al.* 1987; Ryan *et al.* 1994).

Measurements of macroscopic currents, inhibitory synaptic currents and radioligand binding assays suggest that the principal effect of this mutation is likely to be a reduction in the receptor sensitivity to glycine (Ryan *et al.* 1994; Saul *et al.* 1994; Mascia *et al.* 1996; Graham *et al.* 2006). In this paper we aim to elucidate the reason for this reduced sensitivity.

Analogy with the crystal structures of the muscle nicotinic receptor (Unwin, 2005) and the homologous molluscan ACh-binding proteins (Brejc *et al.* 2001; Hansen *et al.* 2004), suggests that the alanine in position 52 lies

 DOI: 10.1113/jphysiol.2006.126920

outside the glycine-binding site, at the edge of loop 2, and therefore at the base of the extracellular agonist-binding domain, just above the important transduction domain of the M2–M3 loop (Colquhoun & Sivilotti, 2004).

With some notable exceptions (for instance Grosman *et al.* 2000; Chakrapani *et al.* 2004; Lee & Sine, 2005), most studies addressing the effect of mutations have been analysed outside the context of an activation scheme. This means that little can be said beyond the observation of a change in agonist potency (EC_{50}). By this criterion, many residues and secondary structure elements have been labelled as 'critical' for activation, but with no inferences being possible about how this happens. It is only by postulating a mechanism, and fitting it to observed single-channel data, that we can go further. Activation mechanisms, based on rational postulates about the conformations that the receptor adopts during activation, can yield information about the number of binding sites, their microscopic properties and the efficacy of channel opening, and this is a critical step in rational drug design.

In this study, we have investigated the single-channel properties of recombinant glycine receptors that carry the A52S mutation known to produce the *spasmodic* hyperekplexia phenotype in mice. We assessed the influence of the mutation on the activation mechanism of the receptor, using maximum-likelihood fitting, in the context of previous studies on the wild-type receptor.

Methods

Heterologous expression of wild-type and mutant rat glycine receptors in HEK293 cells

Human embryonic kidney cells (HEK293, ATCC, ATCC-CRL-1573) were maintained at 37°C in a 95% air 5% CO_2 incubator in Dulbecco's modified Eagle's medium supplemented with 0.11 g l^{-1} sodium pyruvate, 10% v/v heat-inactivated fetal bovine serum, 100 U ml^{-1} penicillin G, 100 μg ml^{-1} streptomycin sulphate and 2 mM L-glutamine (all from Gibco.Brl, UK) and passaged every 2–3 days, up to 20 times.

Cells were plated on 35 mm culture dishes, incubated for 10 h and then transfected by a calcium phosphate–DNA coprecipitation method (Groot-Kormelink *et al.* 2002) with cDNAs for the rat α1 or for both the α1 and β glycine receptor subunits. For the amplification and cloning of the rat α1 (GenBank accession number AJ310834) and β (GenBank accession number AJ310839) GlyR subunits into the pcDNA3.1(+) vector (Invitrogen, the Netherlands), see Beato *et al.* (2002) and Burzomato *et al.* (2003), respectively. The A52S mutant in α1 (where A stands for alanine and S for serine, respectively) was created using the QuikChange Site-Directed Mutagenesis Kit (Stratagene). The full-length coding sequence of α1A52S was verified by sequencing to check for PCR artefacts.

Each dish was transfected with a total of 3 μg of cDNA. In all cases, 0.3 μg of the marker Enhanced Green Fluorescent Protein plasmid (EGFP-c1, Clontech, UK) was cotransfected in order to allow detection of transfected cells. For heteromeric transfections, the balance of cDNA was that coding for the α1A52S subunit and the β subunit. The latter was included in 40-times greater quantity in order to minimize contamination by homomeric α1 receptors (Burzomato *et al.* 2003). Very few homomeric receptors were formed under these conditions, and currents originating from these receptors were discerned (in most but not all cases, see Results) due to their large amplitude, and omitted from the analysis of heteromeric patches. For homomeric transfections, 5–20% of the transfected DNA was that coding for the α1A52S subunit, and the remainder was empty vector, as described by Groot-Kormelink *et al.* (2002).

Single-channel electrophysiology

Data were collected at room temperature (21°C), 1–3 days following transfection, in the cell-attached patch configuration. The cells were bathed in extracellular solution composed of (mM): NaCl, 102.7; $MgCl_2$,1.2; $CaCl_2$, 2; KCl, 4.7; glucose, 14; Na gluconate, 20; sucrose, 15; TEA·Cl, 20 and Hepes, 10 (pH adjusted to 7.4 with NaOH). The pipette solution was identical, with glycine added (30–10000 μM for heteromers, and 30–50000 μM for homomers). In order to avoid increasing the osmolarity of the pipette solution excessively at high agonist concentrations, glycine was added from a stock solution equi-osmolar with the extracellular solution, composed as follows (mM): glycine, 100; NaCl, 80; Hepes, 10 (pH to 7.4 with NaOH). Thick-walled borosilicate glass pipettes (GC150F, Harvard Instruments) were coated with Sylgard 182 (Dow Corning), and polished to a final resistance of 8–15 MΩ.

Given that we record in cell-attached mode, the external chloride concentration is fixed by the extracellular solution in our patch pipette. The amplitude of glycine channel openings is determined by the internal chloride concentration (on which the conductance of the channel depends, Bormann *et al.* 1987), and the resting membrane potential of the cell (which contributes to the driving force together with the pipette potential which we clamp). As both are unknown, vary from cell to cell, and were beyond our control in the cell-attached configuration, variability in glycine channel amplitude was observed between patches. Following formation of a gigaseal, the membrane was hyperpolarized by setting the pipette voltage to 70–110 mV, choosing the holding voltage in such a way as to reduce the spread of channel amplitudes between experiments (Beato *et al.* 2004; Burzomato *et al.* 2004). In certain patches, glycine receptor activations could be clearly observed when the pipette voltage was

held at 0 mV, suggesting that the cell had a particularly negative resting membrane potential. In this case, the pipette voltage was set to the low end of the working range (around 80 mV) in order to avoid excessive hyperpolarization, which tends to shorten the life of patches.

Our aim was to keep the transmembrane voltage as uniform as possible across patches. The kinetics of heteromeric glycine receptors are known to be moderately voltage dependent: a change of ±15 mV in the transmembrane potential produces a ±10% change in the time constant of deactivation (Gill *et al*. 2006). In the patches used for further analysis, we observed no differences in the behaviour of glycine receptors over a range of pipette voltages (−80 to −120 mV). In about 5% of patches, glycine channels had a small amplitude (i.e. less than 2.5 pA at a pipette voltage of 100 mV) and a shallow *I–V* relation (presumably due to a low internal chloride concentration); these patches were discarded.

In order to ensure a high signal to noise ratio, and permit a temporal resolution (30 μs) sufficient for observing the brief shuttings that predominate at higher glycine concentrations, only patches where r.m.s. baseline noise was less than 280 fA (5 kHz bandwidth, i.e. the reading from the Axopatch amplifier meter) were analysed. Low-noise recording was aided by holding the pipette at a steep angle and keeping the bath solution only a few hundred micrometres deep, in order to minimize the immersion of the pipette tip (Benndorf, 1995). The current output of the patch-clamp amplifier, prefiltered at 10 kHz (Axon Instruments 200B, Molecular Devices, USA), was recorded on digital tape (Biologic 1204, France). For acquisition off-line, the signal was filtered at 3 kHz using an 8-pole Bessel filter, and acquired at 40 kHz via an A/D interface (Axon Instruments 1322) using Clampex (Axon Instruments). All programs used in our analysis can be obtained from http://www.ucl.ac.uk/Pharmacology/dc.html.

Following idealization of the channel records using time-course fitting with SCAN (Colquhoun & Sigworth, 1995) into sequences of 10000–25000 transitions, data were first analysed using empirical fits to amplitude and dwell-time histograms by the program EKDIST. We observed only one conductance level in all recordings (after omitting occasional homomeric openings), so the amplitude histogram was fitted with a single Gaussian. Only amplitudes longer than two filter rise times (220 μs at 3 kHz) were included in the amplitude histogram. Open and shut dwell-time histograms were fitted with a mixture of exponential densities. The reason for this initial fitting of dwell-time distributions was to determine the critical time for dividing recordings into groups of openings and shuttings that are likely to arise from the activity of one individual channel, i.e. into activations (bursts) or groups of activations (clusters). We did not use the time constants estimated from the dwell-time histograms or the channel amplitudes for any further analysis.

Activations recorded at 30 μM glycine were divided into bursts. However, the results of this procedure were ambiguous due to the poor separation of bursts. Shut times within bursts were longer in the mutant than in wild-type channels, but in records where the bursts were well separated enough to allow unambiguous determination of the critical time (i.e. those with few channels in the patch), we were not able to observe enough transitions (a problem similar to that described by Beato *et al.* 2002). Recordings made at 100, 300, 500, 1000, and 10000 μM glycine were divided into clusters by empirical determination of the critical shut time. A resolution of 30 μs was imposed retrospectively on the idealized data.

Single-channel open-probability–concentration curve

At glycine concentrations greater than 30 μM, heteromeric channel openings occurred in clusters separated by long quiescent periods, which are likely to be sojourns in long-lived desensitized states. Only clusters that did not contain double openings were selected for further analysis (33–471 clusters analysed per concentration; clusters contained up to 3555 openings, and the mean number of openings per cluster was 522). Each of these clusters is likely to represent the activity of a single glycine channel (Sakmann *et al.* 1980; Burzomato *et al.* 2004).

For each patch (three to five per concentration; see Table 4), the probability of being open (P_{open}) was estimated as the ratio between the total open time and the total duration of the clusters. Both quantities were obtained from the idealized record. This procedure effectively weights the contribution of each cluster to the P_{open} value according to its duration, because P_{open} estimates derived from the longer clusters are more precise. For this reason, no clusters were omitted on the arbitrary basis of not containing enough events. Those that contained few events occupied a small proportion of the total time, and hence made little contribution to the estimate. These values were averaged and fitted with the Hill equation (least squares fit with weights from the standard deviation of the means at each concentration) using the CVFIT program. This Hill slope was compared with that predicted by fitted mechanisms. The latter will not have constant Hill slopes, so the Hill slope at EC_{50} (defined in this case as the tangent to the predicted concentration dependence of P_{open} on concentration), was found numerically.

$$n_{\text{H50}} \equiv \left. \frac{\mathrm{d} \ln \left(\dfrac{P_{\text{open}}}{P_{max} - P_{\text{open}}} \right)}{\mathrm{d} \ln(G)} \right|_{G=\text{EC}_{50}}, \qquad (1)$$

where G is the glycine concentration.

Maximum-likelihood fitting

Several postulated mechanisms were evaluated by maximum likelihood fitting using the HJCFIT program. Idealized recordings of 12–24000 transitions from single patches were formed into four sets for simultaneous fitting. Each set consisted of data from three patches, one at each concentration of glycine (300, 1000, 10000 μM). Ten patches were used in total (see below; two were used twice, i.e. in two sets). The resolution (the duration of the fastest events that can be unfailingly detected, in our case 30 μs) was imposed retrospectively on the idealized data by the HJCFIT program according to the HJC definition (Hawkes *et al.* 1990, 1992) and used for exact missed event correction. Openings were divided into groups using a critical shut time (t_{crit}), which was defined so that the openings within each group are likely to come from the same channel. Activations from contiguous stretches of patch recording (sections with seal breakdowns or other noise were skipped) were grouped into 10–30 clusters per patch. Only shut times shorter than t_{crit} are used for fitting, longer shut times being unusable when the number of channels in the patch is unknown.

The likelihood of each group was calculated using the initial and final steady-state vectors. We were unable to estimate the true initial vector because the gaps between clusters arose from long-lived desensitized states that we do not include in our mechanisms. Using the steady-state vectors is an approximation, but not an important one, because the number of events in our groups was typically large, and this has been shown to minimize the effects of any errors in the initial vector (Colquhoun *et al.* 2003).

In principle, the set of data to be fitted should be obtained at a range of concentration that is such as to contain information on all parts of the mechanism, including the different binding steps (Colquhoun *et al.* 2003). This is best achieved when low-concentration data (where groups of openings are likely to be single activations of the receptor and lower levels of ligation will be more represented) are fitted simultaneously with high-concentration data (where clusters of activations are seen). Most of our fits were done by fitting simultaneously recordings made at three different glycine concentrations with a single set of rate constants. In order to get good fits, we had to omit results at the two lowest concentrations (30 and 100 μM glycine), and a couple of patches at higher concentrations. This may be a consequence of receptor heterogeneity of the expressed receptors and/or because the postulated mechanism was inadequate (see Results and Discussion).

Each fit was repeated using several different initial guesses. If the likelihood surface has a well-defined maximum, the same estimates for the rate constants should be obtained, independently of the initial guesses, if the fit converges.

At the end of the fit, the approximate standard deviation of the estimates was estimated from the local curvature (approximate second derivative) of the likelihood surface, as calculated from the Hessian matrix. At the peak in the likelihood surface, changing a well-defined parameter should result in a reduction in the likelihood. This enabled a gross assessment of the accuracy of the fit, because parameters that were not well defined had little effect on the likelihood when altered. Fits where rates were not defined in this manner were discarded. In general, this occurred most commonly when fitting mechanisms that had a large number of free parameters (i.e. 20 or more), and indicates the limit of the number of parameters that could be satisfactorily estimated from our data (typically 18, similar to Burzomato *et al.* 2004).

To test the adequacy of fits where all the rates were well defined, the predictions of the mechanism together with the rate constants estimated by maximum-likelihood fitting were compared with the experimental observations using four types of data display: the open and shut dwell times, the mean open times conditional on the adjacent shut interval, and the P_{open}–concentration curve (see Burzomato *et al.* 2004 for a detailed discussion of the construction and interpretation of these plots).

All data are expressed as mean ± S.D. of the mean. For estimated rate constants we report the mean of estimates obtained from different sets and the coefficient of variation (CV) of the mean. Figure 10 was prepared with Pymol (DeLano Scientific, USA) from Protein Data Bank file 2BYN (Hansen *et al.* 2005).

Results

We recorded both heteromeric (containing both α1 A52S and β subunits) and homomeric (α1 A52S) glycine receptors in the cell-attached configuration over a wide concentration range (10–10000 μM for A52S heteromeric and 100–50000 μM for A52S homomeric). Before discussing fits, it is necessary to consider some experimental problems.

Heterogeneity of expressed receptors

It is quite a common problem in single-channel work on recombinant receptors that the expressed receptors are not all identical. This sort of heterogeneity will presumably also affect results with whole-cell currents, but will not be so immediately noticeable unless the heterogeneity is gross. The greater discriminating power of single-channel measurements reveals even small amounts of heterogeneity, and that is important for our analysis.

Heterogeneity can be detected most easily at high agonist concentrations, where long clusters of activations can be seen, separated by desensitized periods. Each cluster

arises from one individual receptor (P_{open} is sufficiently high within the cluster that it is obvious if a second channel becomes active, as in Fig. 1*C*, bottom trace).

Heteromeric αA52S receptors were often homogenous. In most patches that we analysed in which channel expression was moderate or low (21 of 25), only a single population of channels was present, as judged by the fact that P_{open} was much the same in all the clusters (Fig. 1*A* and *B*). However, at high levels of receptor expression, where more than one channel in the patch was regularly active simultaneously (as was often observed on the second or third day following transfection), we observed more than one type of channel activity as determined by the cluster P_{open} (Fig. 1*C* and *D*). The channel amplitude was the same for each type, which ruled out contamination by homomeric channels, but the shut time distributions were quite different.

One type of cluster seemed similar to those seen in the homogeneous recordings, whereas the other had a lower P_{open}. Patches with this sort of heterogeneity, and patches with many doubles, were discarded. At lower concentrations of glycine, where heterogeneity was harder to detect on the basis of P_{open}, we used only patches from cells showing low expression where few double openings were seen.

Homomeric αA52S receptors showed more serious problems of heterogeneity. Unlike with the heteromeric receptor, we saw mixed populations of receptors (as assessed by cluster P_{open}) in the same patch, and different types of consistent activity between different patches on the same day. The level of expression was generally low for this receptor, and we did not observe consistent patterns dependent on the time elapsed from transfection of the cells, as for the heteromeric type. We were not able to estimate the maximum P_{open} of the receptor because we observed similar behaviour at 10, 50 and 100 mM glycine, with cluster P_{open} ranging from 75% to 99%. We suspected that this behaviour could be due to contaminant zinc, which enhances macroscopic responses of glycine receptors at submicromolar concentrations (Miller *et al.* 2005) and may be present at sufficient levels in our salts (Wilkins & Smart, 2002). We tested for the possibility that zinc could increase the receptor P_{open} for long periods before unbinding, producing clusters where P_{open} would vary. Hence, we included EDTA (2 mM) in our solutions to chelate zinc to femtomolar levels, and elevated the total calcium to 2.25 mM (in order to maintain the same level of free calcium). But in these experiments, cluster P_{open} remained mixed between and within patches ($n = 5$). We have excluded homomeric data from further analysis.

Empirical fits

Clustered groups of activations separated by long sojourns (1–200 s) in desensitized states (Sakmann *et al.* 1980) were observed in all patches from cells expressing heteromeric

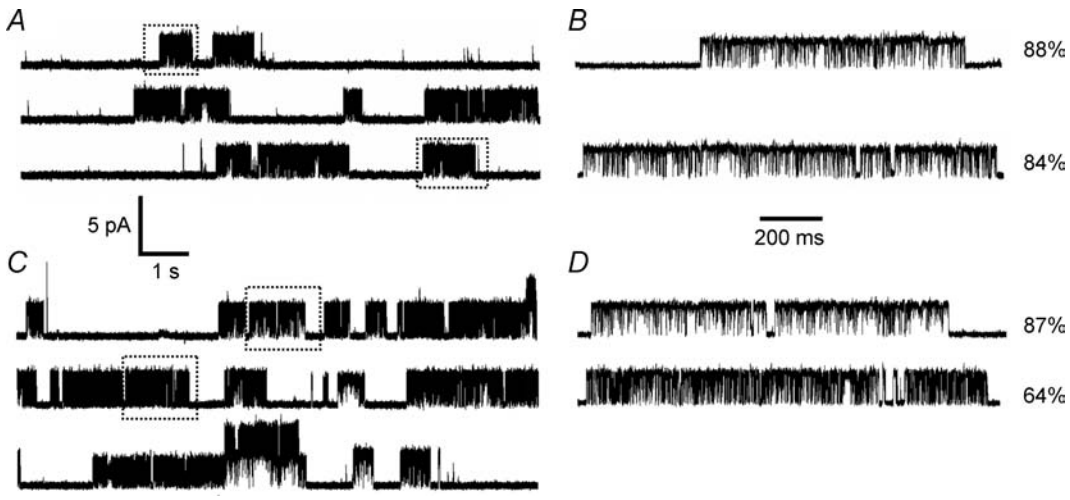

Figure 1. Heterogeneous and homogeneous clusters of α1 A52S-β heteromeric receptor activations recorded in 1 mM glycine
A, when expression of the receptor was low enough to see only isolated single clusters, the P_{open} of each cluster was very consistent within patches and between patches. *B*, two clusters separated by about 25 s, and indicated by boxes in *A*, are shown on an expanded scale. The other clusters in the patch were similar. No double activations were seen in this patch. *C*, in a patch where more than one channel was typically active, which was typical of patches recorded more than two days after transfection of the cells, large variability of cluster P_{open} was observed, with two or more apparent populations. *D*, two representative clusters, indicated by boxes in (*C*), with very different open probabilities. One population (upper trace) seemed to display an open probability similar to that observed in the homogeneous recordings. Patches that demonstrated this kind of heterogeneous mixture of clustered activations were discarded. The data were filtered at 3 kHz.

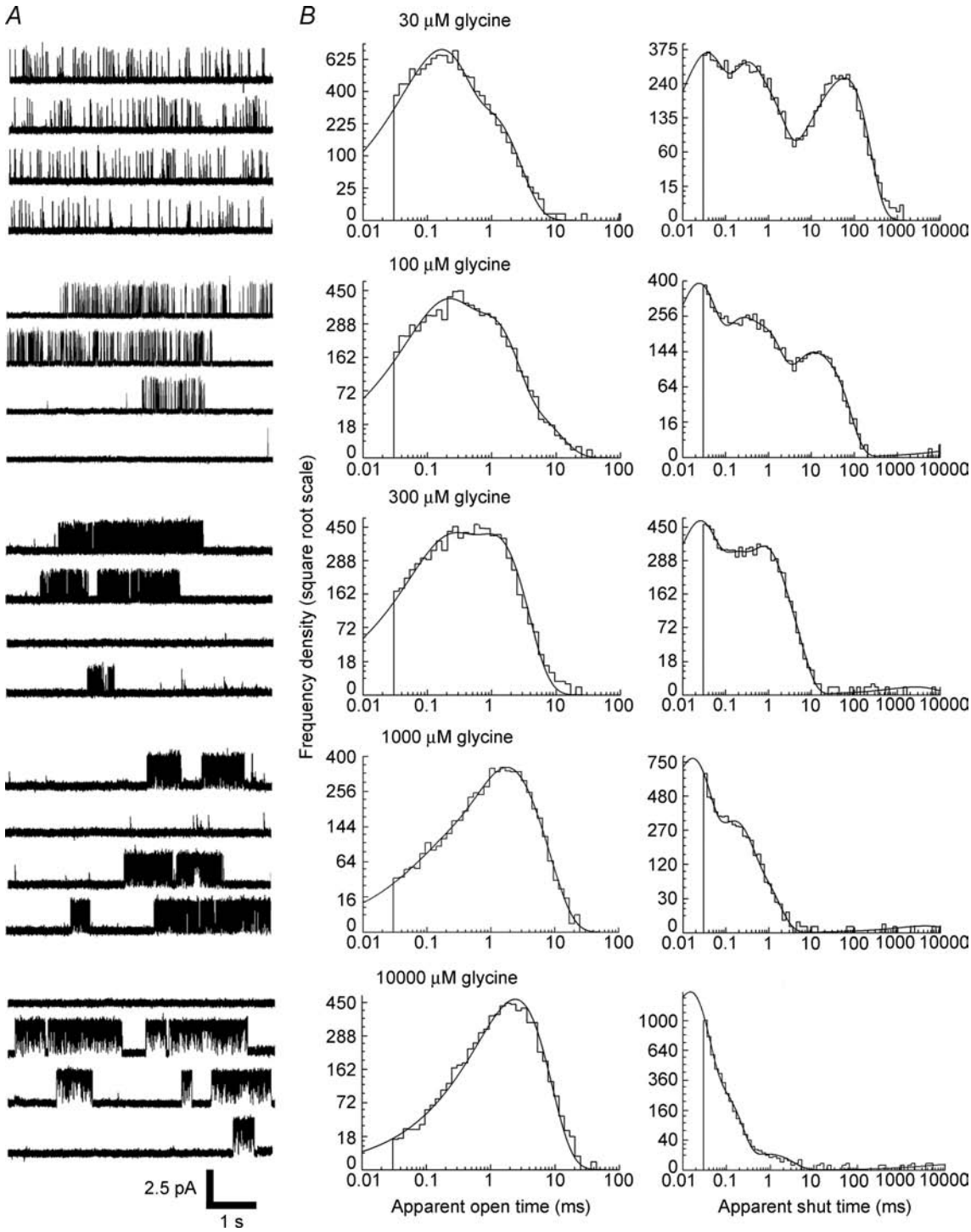

Figure 2. Activation of heteromeric α1 A52S-β receptors by increasing concentrations of glycine
A, raw data traces are at five concentrations of glycine on heteromeric α1 A52S-β receptors. Bursts of openings occur at 30 μM glycine, but at higher concentrations, these activations group into clusters. *B*, the empirically fitted dwell-time histograms show that at low concentration, an appreciable proportion of openings are too fast to be observed. At higher concentrations of glycine, the apparent open time lengthens, mainly because the number of short shuttings that are missed increases progressively with glycine concentration. The predominant fast shut time observed in wild-type receptors is similar for A52S, but less pronounced. The longer intracluster shut times that are observed at low concentrations probably represent unbinding and rebinding of agonist, because they gradually shorten as the receptor becomes progressively more heavily liganded at higher concentrations of glycine. At the highest concentration, when the receptor is saturated with agonist, these longer shut times all but disappear.

Table 1. Empirical fit of mixtures of exponential densities to the distributions of apparent open times from αA52S receptors

Gly (μM)	*n*	τ_1 (ms) (area (%))	τ_2 (ms) (area (%))	τ_3 (ms) (area (%))
30	4	0.13 ± 0.01 (68 ± 3)	0.72 ± 0.04 (32 ± 3)	
300	4	0.16 ± 0.01 (40 ± 2)	1.1 ± 0.1 (60 ± 2)	
1000	5	0.13 ± 0.01 (12 ± 2)	1.2 ± 0.1 (58 ± 7)	3.4 ± 0.4 (30 ± 7)
10000	4			3.4 ± 0.5 (100)

Time constants and areas are expressed as mean $\pm$ S.D. of the mean.

Table 2. Empirical fit of mixtures of exponential densities to the distributions of apparent shut times from αA52S receptors

	Apparent shut times					Mean shut time (ms)	
Gly (μM) (*n*)	τ_1 (ms) (area (%))	τ_2 (ms) (area (%))	τ_3 (ms) (area (%))	τ_4 (ms) (area (%))	τ_5 (ms) (area (%))	Within cluster	Within burst
30 (4)	0.020 ± 0.003 (30 ± 4)	0.13 ± 0.037 (20 ± 2)	0.67 ± 0.10 (19 ± 2)	15 ± 3 (13 ± 13)	65 ± 11 (19 ± 10)		0.16 ± 0.02
300 (4)	0.023 ± 0.005 (30 ± 2)	0.12 ± 0.063 (23 ± 2)	0.56 ± 0.12 (22 ± 2)	2.6 ± 0.4 (24 ± 2)	1700 ± 400 (0.08 ± 0.01)	0.88 ± 0.06	
1000 (5)	0.017 ± 0.002 (67 ± 3)	0.11 ± 0.02 (20 ± 1)	0.38 ± 0.02 (12 ± 2)	2.8 ± 0.4 (0.4 ± 0.1)	9000 ± 2000 (0.09 ± 0.01)	0.091 ± 0.010	
10000 (4)	0.013 ± 0.001 (76 ± 8)	0.069 ± 0.012 (22 ± 8)		1.6 ± 0.7 (1.1 ± 0.5)	2100 ± 1100 (0.12 ± 0.04)	0.034 ± 0.007	

Time constants and areas are expressed as mean $\pm$ S.D. of the mean. The critical shut times for dividing bursts (at 30 μM glycine) and clusters (at all other concentrations) were, in ascending order of concentration: 4, 30, 20 and 15 ms.

A52S glycine receptors, at concentrations above 30 μM. The mean channel amplitude was similar to that observed in wild-type heteromeric receptors (3.8 ± 0.1 pA, $n = 31$), as expected from the slope conductance of 39 pS reported by Burzomato *et al.* (2003). The distributions of apparent open and shut times were fitted with mixtures of exponential distributions. They are shown in Fig. 2.

The open time distributions were fitted well by up to three components (see Table 1). The fits summarized in Table 1 show that the mean apparent open time increased with glycine concentration. At the highest concentration, when most receptors should be fully liganded, a single exponential fitted well (as for the nicotinic receptor, e.g. Hatton *et al.* 2003; Fig. 4*A*). The shut time distributions (Table 2) were fitted with up to five components. The fastest component of the shut time distribution (13–20 μs) was comparable with that seen for wild-type receptors (12–15 μs, Burzomato *et al.* 2004).

At the lowest concentration of glycine that we examined (10 μM), we did not observe bursts of full-amplitude channel activations. Any ambiguous activity was also very sparse (less than 100 transitions per patch) and so did not yield enough transitions for further analysis. At 30 μM (Fig. 2*A* and *B*), most channel activations were short and the open time distribution suggested that some openings were too short to be detected. Because many openings did not reach full amplitude, it was difficult to determine whether the receptor population was made up of only one type of channel (as determined by a consistent amplitude), and contamination by homomeric channels or other forms of the receptor could not be ruled out. Indeed, the shut-time distributions were rather variable at this concentration. These two findings highlight a difficulty in working with loss-of-function mutations, because our methods depend on unambiguous resolution of well-separated bursts which reach full amplitude, such as observed with wild-type glycine or nicotinic receptors. This is needed not only for profitable kinetic analysis, but also to exclude contamination of the record with extraneous activations from a mixed population of channels.

Dwell-time distributions were fitted with mixed exponential densities; the number of components is the same as summarized in Tables 1 and 2. The number of components required to fit the open and shut times observed at 100 μM glycine were three and five, respectively. Open-time distributions at 30, 100, 300, 1000 and 10000 μM glycine include 10480, 7561, 8430, 5582 and 4693 openings, respectively. Shut-time distributions include (in the same order): 10480, 7562, 8431, 5583 and 4694 shut times.

Figure 3 shows the distributions of the lengths of bursts of openings at low agonist concentrations, at which bursts should be a good approximation to individual channel activations. Wild-type and αA52S mutant receptors were recorded at glycine concentrations that were roughly equi-effective in eliciting macroscopic responses (about 5% of maximum), 10 and 30 μM , respectively.

The mean burst length was shortened by the αA52S mutation. The slowest component of the burst length distribution, which is what usually determines the decay rate of synaptic currents, is about five times faster for the mutant receptor than for wild type (see Table 3).

Figure 3*C* and *D* shows examples of the distribution of the probability of being open within a burst for these low concentration experiments. For the wild-type receptor, the distribution is similar to that predicted from the fit of the flip mechanism in Burzomato *et al.* (2004). The rates estimated there were used to simulate data (program SCSIM, and the distribution of P_{open} was plotted in EKDIST, data not shown). Thus, the flip model describes the wild-type data and there is no evidence of heterogeneity. But for αA52S, the distribution of burst P_{open} (Fig. 3*C*) was much more evenly spread than predicted, on the basis of data simulated with the rates from the fit shown in Fig. 9 (data not shown). There are two possible reasons for this. One is heterogeneity of the receptors (which cannot be detected directly in low-concentration experiments). Another possibility is that the mechanism being fitted is inadequate to describe the data. There is no way to distinguish these two possibilities unambiguously, but it is hard to imagine a mechanism that would predict the sort of flat distribution seen in Fig. 3*C*, so heterogeneity seems a more likely explanation. For this reason the lowest-concentration records had to be excluded for fits.

Single-channel P_{open}–concentration response curve

We constructed a plot of P_{open} values clusters measured from patches at five concentrations of glycine (100 μM –10 mM, Table 4), at which clear clusters of openings

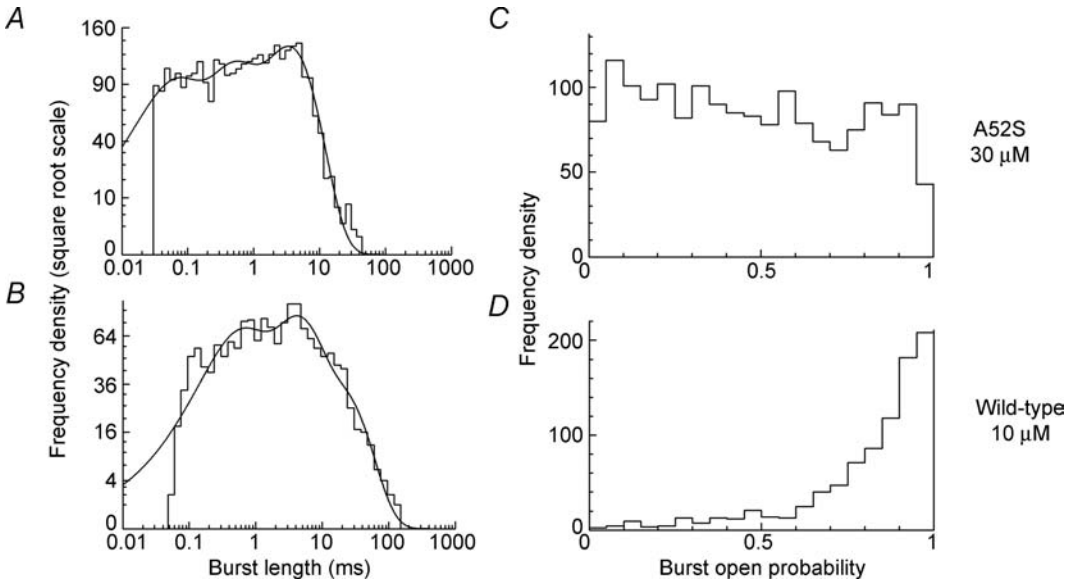

Figure 3. Properties of bursts for wild-type and α1A52S mutant heteromeric glycine receptors
A, a typical burst-length distribution for α1-A52S-β heteromeric glycine receptors at 30 μM glycine. *B*, the same distribution for wild-type heteromeric receptors, using the data of Burzomato *et al.* (2004) is plotted for comparison at 10 μM glycine, a concentration equi-effective in terms of P_{open}. The burst-length distributions are fitted with a mixture of exponential densities, with three components in each case (see Table 3). In comparison with wild type, A52S records show a much smaller proportion of long bursts (that is, those longer than 10 ms) and many more short bursts, the fastest of which arise from isolated single apparent openings. The critical time for dividing the record into groups of openings arising from a single channel was 4 ms for both datasets. This choice was unambiguous in the case of the wild type, but not for A52S (see Fig. 2 and text). This certainly resulted in a large number of misclassified bursts for A52S. The histogram for αA52S includes 3316 bursts and the parameters were $\tau_1 = 0.06$ ms (area 27%), $\tau_2 = 0.4$ ms (area 25%), $\tau_3 = 3.4$ ms (area 48%). The wild-type histogram contains 1598 bursts, and the fitted parameters were $\tau_1 = 0.4$ ms (area 32%), $\tau_2 = 3.4$ ms (area 44%), $\tau_3 = 17$ ms (area 24%). The burst P_{open} distribution for αA52S (*C*) is unusually flat, which was not predicted by any mechanism we fitted (see Results).Wild-type bursts of openings, contrastingly, had P_{open} (*D*) that was strongly skewed towards the maximum value, much as predicted from simulations. It is not possible to calculate the P_{open} for bursts that consist of a single opening, so these were excluded. The total number of bursts plotted in these histograms are (for A52S, *C*) 1702 and (for wild-type, *D*) 898.

Table 3. Empirical fits to distributions of burst lengths

	Mean ± S.D of the mean (ms)	Mean area ± S.D of the mean (%)
αA52S		
τ_1	0.07 ± 0.01	38 ± 4%
τ_2	1.0 ± 0.4	33 ± 5%
τ_3	4 ± 1	29 ± 8%
Wild type		
τ_1	0.6 ± 0.2	33 ± 4%
τ_2	4.0 ± 1	46 ± 4%
τ_3	22 ± 3	21 ± 5%

Means of four patches for both wild-type (data from Burzomato 2005) and αA52S heteromeric receptors, glycine 10 and 30 μM, respectively. The critical shut time for dividing bursts was 4 ms in each case. The fastest time constants will arise largely from isolated openings. The fact that they differ somewhat from the fastest time constant of the open-time distribution results partly from experimental error and partly because the distribution in this region is not in principle described by the mixture of exponentials fitted here (Hawkes *et al.* 1990, 1992; see also discussion in Burzomato *et al.* 2004). The slow component of the burst-length distribution found by Burzomato (2005) (22 ms) seems to be longer than that predicted from the model and rates at 10 μM (11 ms, not shown). The latter is longer than the predominant current decay (6 ms) because 10 μM is not a sufficiently low concentration to reach the low concentration limit.

were recorded. Figure 4 shows the activations of A52S heteromeric receptors at the beginning of clusters at each of the five concentrations.

The data (Fig. 4*B*) were fitted empirically with the Hill equation. Although the Hill equation does not describe a plausible activation mechanism, and thus is not the correct equation to fit to the data, it allows us to describe the dose–response curve in terms of the concentration of glycine required to elicit a half-maximal response, and to estimate the steepness of the concentration dependence of the receptor response to glycine near its midpoint. It also allows extrapolation to estimate the maximum P_{open}, though extrapolation with the wrong equation is necessarily dubious. Thus the Hill equation fit allows a rough comparison with previously reported macroscopic data for this mutant receptor.

The fitted maximum P_{open} for the A52S heteromeric receptor was 97% (two-unit likelihood interval from residuals 97–98%), very similar to that measured in the same way for the wild type (98%), which suggested that the efficacy of receptor gating when saturated with agonist remains high (at least 25). The EC_{50} value is however, more than five-fold increased in the A52S receptor, compared with wild-type receptors, to 339 μM glycine (two-unit likelihood interval 309–370, cf. 60 μM for wild type). Ryan *et al.* (1994) reported a similar shift for macroscopic current responses for homomeric mouse receptors containing the A52S mutation, a six-fold increase compared with wild type (mouse α1 is identical with rat α1). However, the shift we observed in the fitted P_{open}–concentration curve is not parallel (if the only effect of the mutation was to change all binding steps equally, the shift would be parallel). The fitted Hill slope of the P_{open} curve for the A52S heteromeric receptor is 2.2 (two-unit likelihood interval 2.0–2.4, Fig. 4). This is less steep than that for the wild-type heteromeric receptor (3.4; two-unit likelihood interval 3.1–3.7; Burzomato *et al.* 2004). There is, in a sense to be explained in the Discussion, a reduced 'cooperativity' in the mutant receptor.

If we constrained the curves to be parallel, a simultaneous fit of the Hill equation to both wild-type and αA52S P_{open} data did not give a satisfactory description of the observed αA52S P_{open} at low concentrations (i.e. the difference between the Hill slope required to give a good fit for WT and αA52S was too large, hence it was underestimated for wild type and overestimated for the αA52S data, data not shown).

The sources of bias in the construction of P_{open}–concentration response curves have been investigated in detail (Burzomato *et al.* 2004).

The shift that we observe in the single-channel P_{open}–concentration response curve (and the shift that had previously been observed in macroscopic data) could arise from either a change in the properties of the glycine binding sites, or a change in the gating of the receptor (this is the classical binding-gating problem, see Colquhoun, 1998).

Radioligand binding experiments cannot resolve this problem, even in the absence of desensitization. The tendency of receptors to accumulate in high-affinity desensitized states poses another problem for ligand-binding experiments, in which agonist exposures are orders of magnitude longer than during synaptic transients or even whole-cell recording electrophysiology. The P_{open}–concentration response curve excludes such long-lived desensitized states when a suitable t_{crit} can be chosen to exclude time spent in desensitized states.

Hence, although previously published data suggest that the A52S mutation does not change ligand binding much (Ryan *et al.* 1994; Saul *et al.* 1994; Graham *et al.* 2006), it cannot be deduced from these studies that the mutation affects only gating, or only conformational changes. These effects can be separated only by postulating a plausible reaction mechanism, so we fitted a number of putative mechanisms to the observed dwell-time sequences, using the maximum-likelihood method (HJCFIT program, Colquhoun *et al.* 1996; 2003).

Fitting mechanisms to the observations

The HJCFIT method (see Methods) was used to fit simultaneously steady-state single-channel recordings

Table 4. Concentration dependence of α1A52S heteromeric glycine receptor cluster length and P_{open}

Gly (μM)	Number of clusters	Number of patches	Cluster length (s)	P_{open} (uncorrected for missed events)
100	33	4	9 ± 2	0.075 ± 0.019
300	54	4	1.5 ± 0.3	0.410 ± 0.033
500	40	3	0.84 ± 0.10	0.672 ± 0.056
1000	84	5	0.67 ± 0.03	0.892 ± 0.008
10000	471	4	0.16 ± 0.02	0.974 ± 0.004

As the glycine concentration increases, the apparent open probability during clusters also increases, and the clusters themselves become shorter. The critical shut times for dividing clusters were 1000, 30, 20, 20 and 0.8 ms for patches recorded at 100, 300, 500, 1000 and 10000 μM glycine, respectively. The critical time was set to a short interval for records at 10000 μM to exclude a small number of longer intracluster shut times (see Results). For the four patches described here, using a longer critical time, 15 ms, resulted in a total number of 117 clusters. In this case, the mean cluster length was 0.69 ± 0.10 s and the P_{open} was 0.962 ± 0.005.

from αA52S heteromeric receptors. The recordings were made at three different glycine concentrations, 300, 1000 and 10000 μM . At these concentrations, clear clustering was observed so it was possible to detect, and discard, records that showed signs of heterogeneity (see above).

Setting the critical shut time (t_{crit}). As mentioned in Methods, the fitting procedure requires that openings be divided into groups using a critical shut time (t_{crit}), such that the openings within each group are likely to come from the same channel. In practice, the choice of t_{crit}

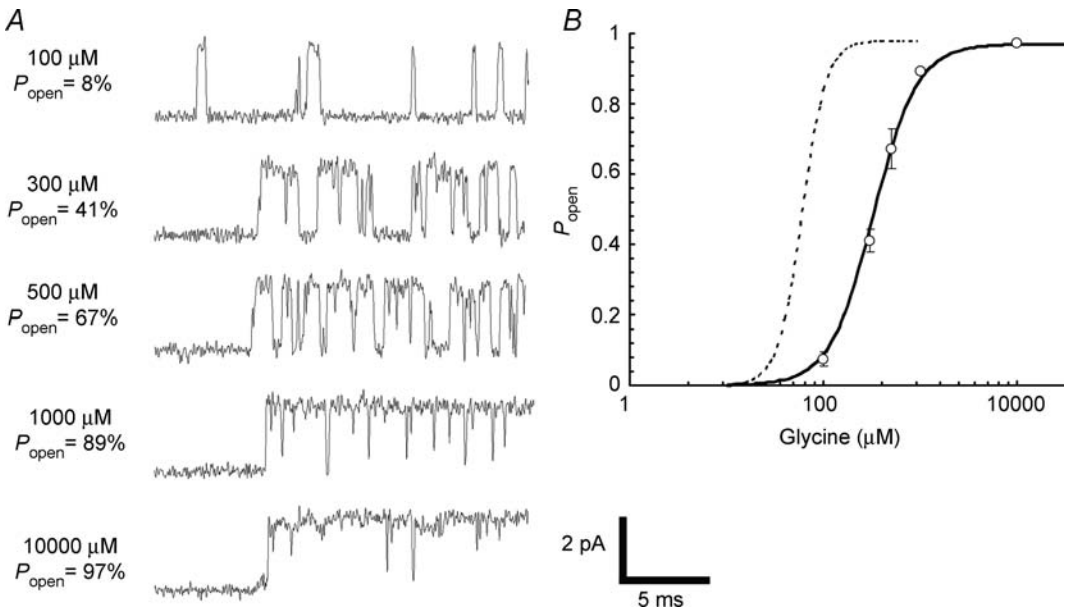

Figure 4. The probability of the channel being open during clusters of α1A52S-β mutant receptor activations

A, expanded view of the beginning of representative clusters for α1 A52S-β heteromeric receptors at five concentrations of glycine. The consistent amplitude of the activations is obvious. Openings are upward. The shortening (and eventual disappearance) of long shuttings within the clusters as the concentration increases is obvious. *B*, the single-channel P_{open}–concentration response relation for A52S heteromeric receptors is shifted to the right, compared with wild-type receptors. The dotted line is a Hill equation fitted to data from wild-type receptors (data from Burzomato *et al.* 2004). Note that the maximum fitted P_{open} is very similar for A52S receptors (97% for A52S, and 98% for wild type), but the Hill slope for the mutant receptor (2.2) is lower than for wild type. Both curves are plotted on an absolute scale, not normalized. Simultaneous fits to wild-type and mutant data with the Hill slope constrained to be the same for each curve did not describe either set of data satisfactorily (data not shown).

is not always obvious. For patches recorded in 300 and 1000 μM glycine, the critical time was set to 30 and 20 ms, respectively, such that only long shut periods between clusters were excluded from fits. But at 10000 μM glycine it was necessary, to get a good fit, to set the critical shut time to 0.8 ms. We chose this rather short value in order to exclude a few longer (1–10 ms) intracluster shut times from fitting. These shut durations are extremely rare compared with the predominant fast shut time component (they constitute only about 1% of the observed shuttings), and hence they do not contribute greatly either to the estimates of P_{open} of the receptor, nor do they have a strong effect on the likelihood calculation. This follows the practice of Beato *et al.* (2004) for the wild-type homomeric glycine receptor. In the past (Beato *et al.* 2004; Burzomato *et al.* 2004) we have displayed the predicted fit to distributions of apparent shut times only up to t_{crit}, on the grounds that shut times longer than t_{crit} are not used for fitting (see Methods). In order to show better what is predicted by the fit and what is not, we now show, in Figs 6, 7, 8 and 9, the data, and the predicted fit, beyond t_{crit} (arrow). The small component of shut times between 1 and 10 ms at the highest glycine concentration (10 mM) cannot be predicted by any of the mechanisms that we tested. It is very unlikely that shut times as short as 1–10 ms could separate clusters of openings that originate from different receptors, at high agonist concentrations, because the channel is open for most of the time and overlapping clusters are relatively rare. It is therefore more likely, that the mechanisms are not quite elaborate enough to predict such minor details.

Mechanisms with two binding sites. Although the stoichiometry of heteromeric receptors remains a matter of debate (Burzomato *et al.* 2003; Grudzinska *et al.* 2005), mechanisms that permit binding of three glycine molecules describe the behaviour of wild-type channels well, and those that include only two do not (Burzomato *et al.* 2004).

This was also the case for the αA52S β receptor, as mechanisms with only two binding sites predicted a Hill slope (at the EC_{50} – see Methods) that was less than 1.5, much shallower than the observed value of 2.2 (Fig. 4). All observed dwell-time histograms were very poorly predicted by such mechanisms, even if extra shut states were included (not shown).

A mechanism with three binding sites that interact. A simple mechanism with three binding sites for glycine which has only a resting state (R) and an open state (R*) for each agonist molecule bound (Scheme 1, Figs 5 and 6*A*) was fitted simultaneously to idealized data at three concentrations (see Methods). The sites were allowed to interact (so the binding was not necessarily the same for the first second and third binding). This mechanism can successfully describe the activation of wild-type homomeric receptors (Beato *et al.* 2004), but is inadequate for wild-type heteromeric receptors, for which additional shut states are required. A similar result was obtained for A52S heteromeric receptors: as shown in Fig. 6.

Although open-time distributions are adequately described by the three open states, the shut-time distributions are not well predicted by this mechanism, as shown by the discrepancy between the continuous lines (i.e. the distributions of dwell times calculated from the results of the global fit of this model to the idealized records and from our experimental resolution) and the histograms (i.e. the observed data). In particular, the fastest shut-time component at 0.3 and 1 mM glycine was badly described, probably because the triply liganded channel shutting rate was consistently underestimated, as was the slope of the predicted P_{open} curve (see Fig. 6*B*).

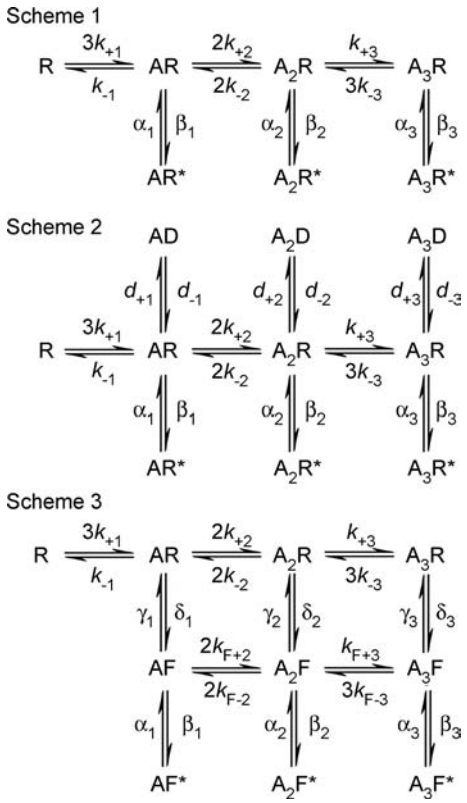

Figure 5. Some of the kinetic schemes that were tested for the αA52S heteromeric glycine receptor
These schemes (and other variants) were previously tested on wild-type $\alpha1\beta$ glycine receptors (Burzomato *et al.* 2004). Agonist molecules (glycine) are indicated by A, and the number bound to each state by a subscript. The resting (shut) states of the receptor are denoted R, and additional shut states either D (desensitized) or F (flipped, i.e. the altered pre-open conformation; see Results). Open states of the channel are indicated by an asterisk (e.g. A_3F^*). The names of the rate constants for the different steps of the reactions are shown, and the statistical factors for the binding rate constants have been included (e.g. the association rate for the vacant receptor is $3k_{+1}$ because any of the three identical binding sites can be occupied).

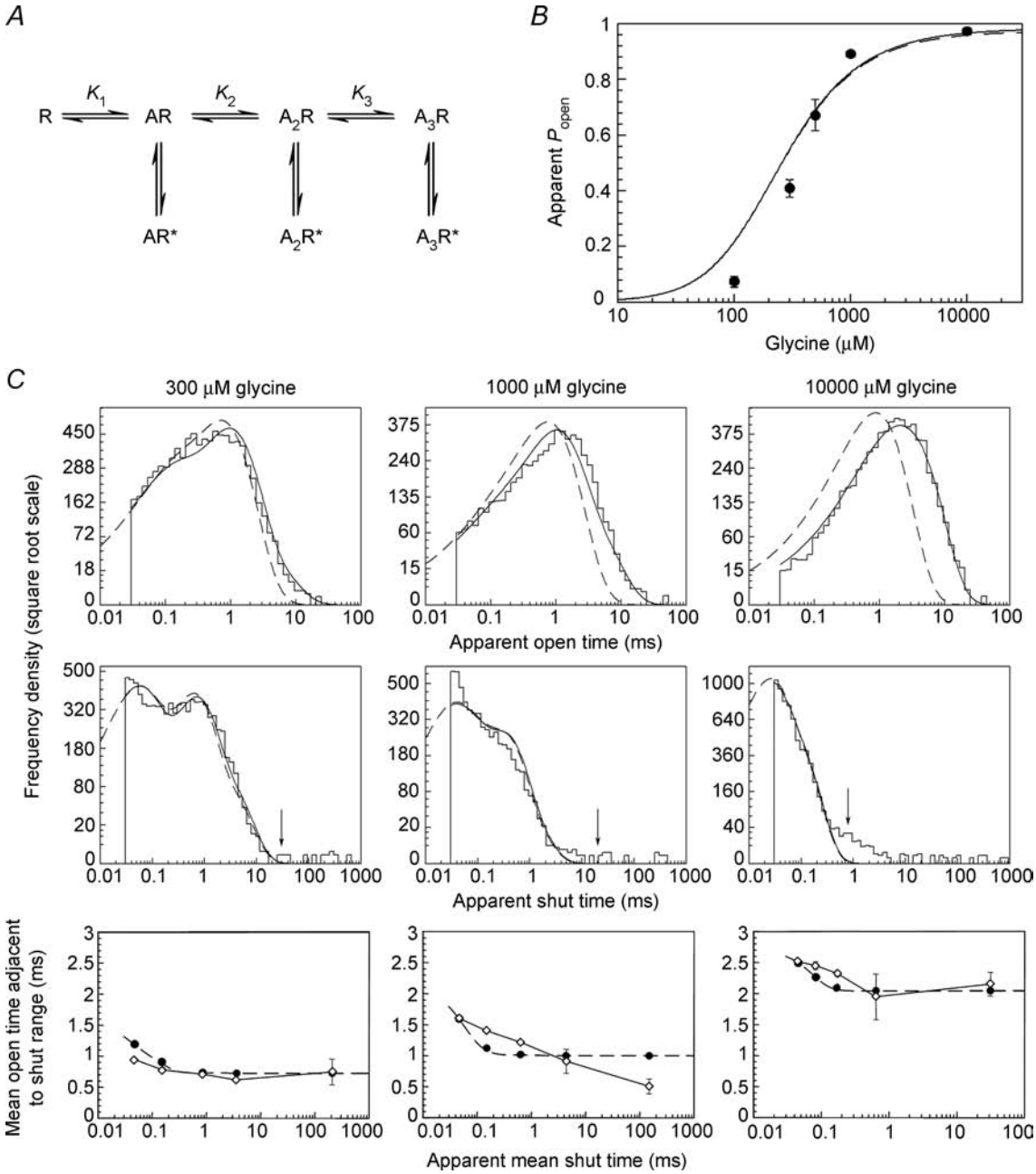

Figure 6. A simple mechanism with three binding sites fails to predict the observed data for the α1A52S-β mutant

A, a simple model for glycine receptor activation, with three binding sites and an open state corresponding to each bound state (Scheme 1 from Fig. 5). *B*, experimental P_{open} values are plotted as filled circles against the glycine concentration. The solid line is the apparent P_{open}–concentration curve predicted by the fitted scheme and rate constants taking into account the effect of missed events. The dashed line is the ideal curve expected if no events were missed. The predicted P_{open}–concentration curve does not describe the observed data, mainly because its slope is too shallow (on average 1.5). These plots indicate that this mechanism describes the data poorly for the αA52S mutant. *C*, all the plots show a comparison of the predictions of the fit with the experimental data. The mechanism was fitted simultaneously to four sets of data at three different glycine concentrations; one of the four sets is shown in this and the other figures. The first two rows of plots show the apparent open- and shut-times distributions. The histograms are the experimental distributions (note that only shut times below t_{crit} are fitted, see Methods). These are the same in Figs 7–9. The open-time histograms at 300, 1000 and 10000 μM include 9034, 6448 and 8002 openings, respectively, and the shut time histograms include (in the same order) 9033, 6447 and 7998 shuttings. The solid lines are predicted (HJC) distributions calculated from the mechanism, the resolution and the values of the rate constants that were found to maximize the likelihood of the experimental sequences of

The arrangement of subunits in the heteromeric receptor suggests that two binding sites are between α and β subunits, and the remaining binding site lies between two α subunits. *A priori*, it seems plausible that the binding sites (and hence their affinity for glycine) may not be identical in the resting state of the receptor, i.e. before they bind the agonist. Nevertheless, mechanisms that presume binding sites to be initially different did not give good fits for either the αA52S data, or for wild-type receptors if they do not allow interaction between the sites.

A mechanism with three binding sites and three extra shut states. Burzomato *et al.* (2004) obtained good fits for the wild-type heteromeric receptor with two activation mechanisms, both of which had an extra shut state for each bound form of the receptor, but differed in the way the shut states are connected. One of these two mechanisms was based on that proposed for the $GABA_A$ receptor by Jones & Westbrook (1995). This has an extra shut state for each level of liganding, and these states can only be accessed from the appropriate closed state as shown in Scheme 2 of Figs 5 and 7*A*. These extra states are labelled, arbitrarily, as desensitized states, but they are really added empirically to get a good fit, and they are too short-lived to account for macroscopic desensitization.

When it is assumed that the three binding sites are independent (so the affinity of each binding site for glycine was the same whether or not other sites were occupied), it was not possible to obtain good fits with wild-type heteromeric data (Burzomato *et al.* 2004), but quite good fits were obtained with αA52S data, as shown in Fig. 7.

The lifetime of the shut state that precedes the fully liganded open state was estimated to be about 14 μs, as expected from empirical fits to the shut time distributions at 10 mM glycine. Correspondingly, the fully liganded channel opening rate (β_3) was around 70 000 s^{-1}, similar to the wild type. The equilibrium dissociation constant for glycine binding to the resting state was about 1.1 mM. However, the A52S P_{open}–concentration response curve predicted by the best fit with this mechanism had a Hill slope at the EC_{50} (1.58 ± 0.05) that was somewhat shallower than measured by fitting the (incorrect) Hill equation, 2.2 (two-unit likelihood interval 2.0–2.4 (see Fig. 4).

When the sites were allowed to interact, a good fit could be obtained for the wild-type heteromeric receptor (Burzomato *et al.* 2004), and in that case the affinity for binding to the resting state appeared to increase strongly for each successive binding step. In the case of the αA52S heteromer, the fit was improved only slightly by allowing interaction, as shown in Fig. 8 (compare with the constrained fit in Fig. 7), despite the fact that the unconstrained fit has four more free parameters (18 rather than 14). The predicted Hill slope at the EC_{50} was slightly larger (1.68 ± 0.08), with the unconstrained fit, so the fit of the P_{open}–concentration curve was slightly better. The fitted rate constants are given in Table 5.

It is now obvious why the fit with the bindings constrained to be the same (Fig. 7) is much better for A52S than for the wild type. The equilibrium dissociation constants for the first second and third binding steps in the unconstrained fit αA52S (Table 5) are $K_1 = 1.4$ mM, $K_2 = 2.1$ mM and $K_3 = 0.62$ mM, none varying greatly from the single value of $K = 1.1$ mM that was found when the sites were supposed to be independent. In contrast, the unconstrained fit to wild-type heteromer (Burzomato *et al.* 2004) gave $K_1 = 14$ mM, $K_2 = 0.2$ mM and $K_3 = 0.01$ mM. Clearly, the apparent 'cooperativity of binding' is greatly reduced in the αA52S heteromer.

The flip mechanism: an explicit pre-opening conformation change with three binding sites that do not interact. Despite the good fit to the data, the Jones and Westbrook-type of model is unsatisfactory in two different ways. Firstly, the fit suggests that as more molecules are bound there is a strong increase in the affinity for binding to the resting conformation for wild-type heteromers (Burzomato *et al.* 2004). This implies that there is a

single-channel openings and shuttings. These distributions allow for missed events on the basis of the imposed resolution, while the dashed lines are the distributions expected if no events were missed. In the third row, the mean durations of openings that are adjacent to shut times in a specified range of duration are plotted against the mean durations of the shut times in each chosen range. The ranges are contiguous; for example in the bottom left panel, the range boundaries are: 30 (the resolution), 100, 300, 2000 and 10000 μs. These plots illustrate the negative correlation between the duration of adjacent open and shut times. Experimental points are shown as open diamonds (±S.D. of the mean) joined by a solid line, predicted points as filled circles, and the theoretical continuous relationship between open time and adjacent shut time as a dashed line. In this mechanism, the affinity of the receptor for glycine varies with the number of binding sites that are occupied. The receptor can open from each bound state, and the resulting three different open states predict the observed open dwell times adequately. But the shut dwell times are not at all well described by this mechanism, and errors in the correlation plots are apparent. In particular, the fastest shuttings are not represented properly, suggesting that additional shut states are required to describe the behaviour of the receptor. For the distributions of apparent shut times (*C*, 2nd row), the value of t_{crit} is shown by a vertical arrow. Only shut times shorter than t_{crit} were used for fitting (see Methods and Results; arrow). The observations, and the predicted fit, are shown for longer shut times to show the small number of 1–10 ms shut times at 10 mM glycine that are not predicted by the fit.

strong interaction between the binding sites. It seems to be unreasonable to imagine that one site would be able to sense whether another site was occupied, given that the sites are a long way apart (at least 40 Å), and no major conformation change has been postulated. Secondly, there is no independent evidence for the existence of the three extra shut states that are introduced in this model, and no knowledge of what their structure might be like, if they do exist. It was these considerations that led Burzomato *et al.* (2004) to postulate an alternative mechanism that is

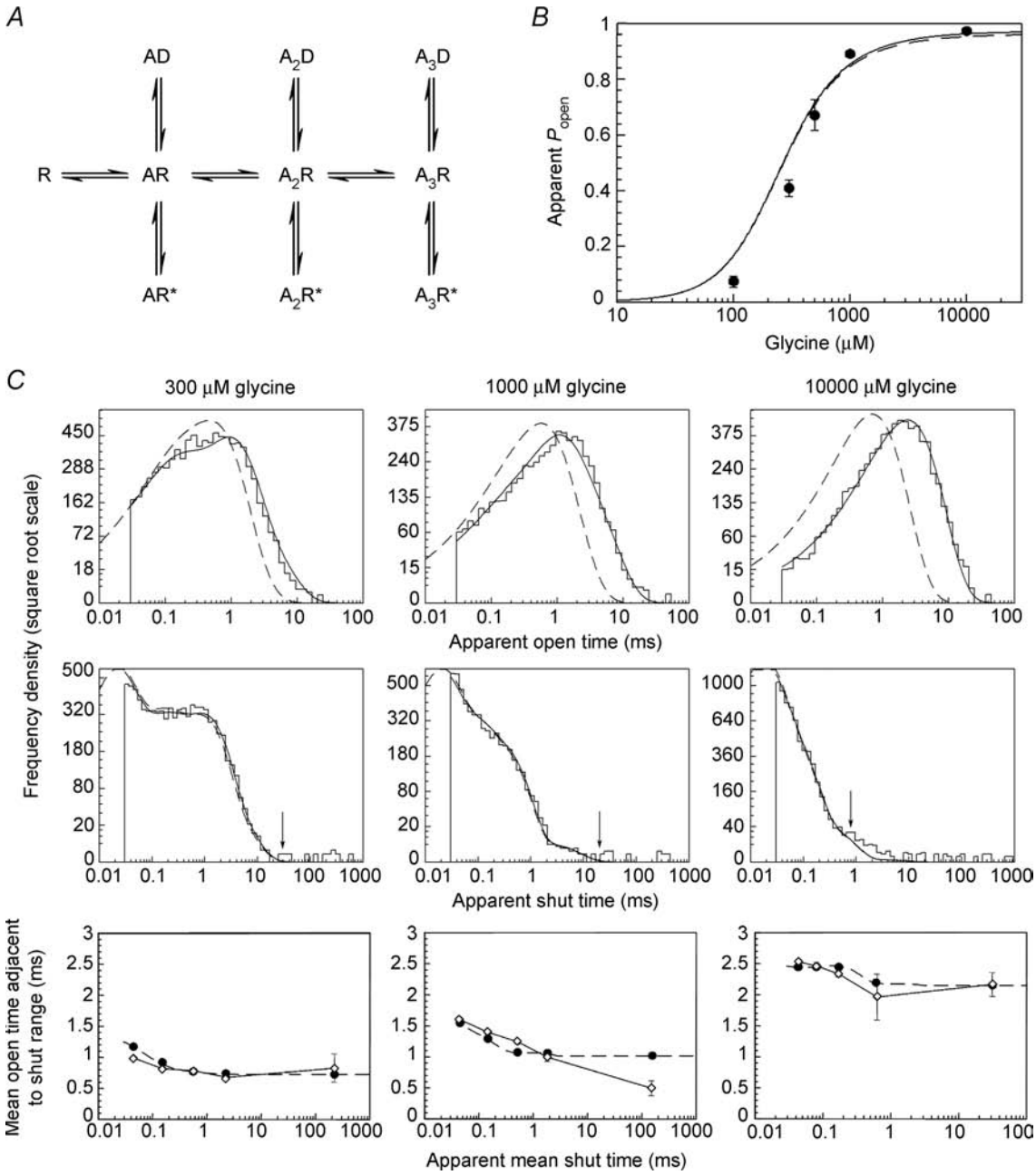

Figure 7. A mechanism that includes three extra distal shut states fits the data well for the αA52S mutant, apart from P_{open}

A, this mechanism (Scheme 2 from Fig. 5) has 14 free parameters, as each binding site is represented as equal and independent. Although some errors are found in the fast components of the shut-time distribution at the lower concentrations (*C*), the dwell times and correlation plots were well described. However, the P_{open}–concentration response curve that this mechanism predicted (*B*) was too shallow to be satisfactory. Only shut times shorter than t_{crit} (arrow in *C*) were used for fitting (see text and Fig. 6 legend) and the (few) 1–10 ms shut times at 10 mM glycine are not correctly predicted by the fit. Of the models that we describe here, this model predicted these shut times somewhat better than the others (perhaps simply because it has the largest number of free parameters), but still not well.

more plausible from the physical point of view. This 'flip' mechanism was based on the following considerations. It is obvious that there must be molecular rearrangements during the process of transduction between the initial ligand binding and the opening of the channel. One obvious example is the domain closure that follows agonist binding, but which may precede opening (Lester *et al.* 2004; Hansen *et al.* 2005). Attempts have been made to map these rearrangements indirectly in the ACh nicotinic receptor (Chakrapani *et al.* 2004), but the possibility remains that intermediate states might be resolved in single-channel recordings for the glycine receptor at least.

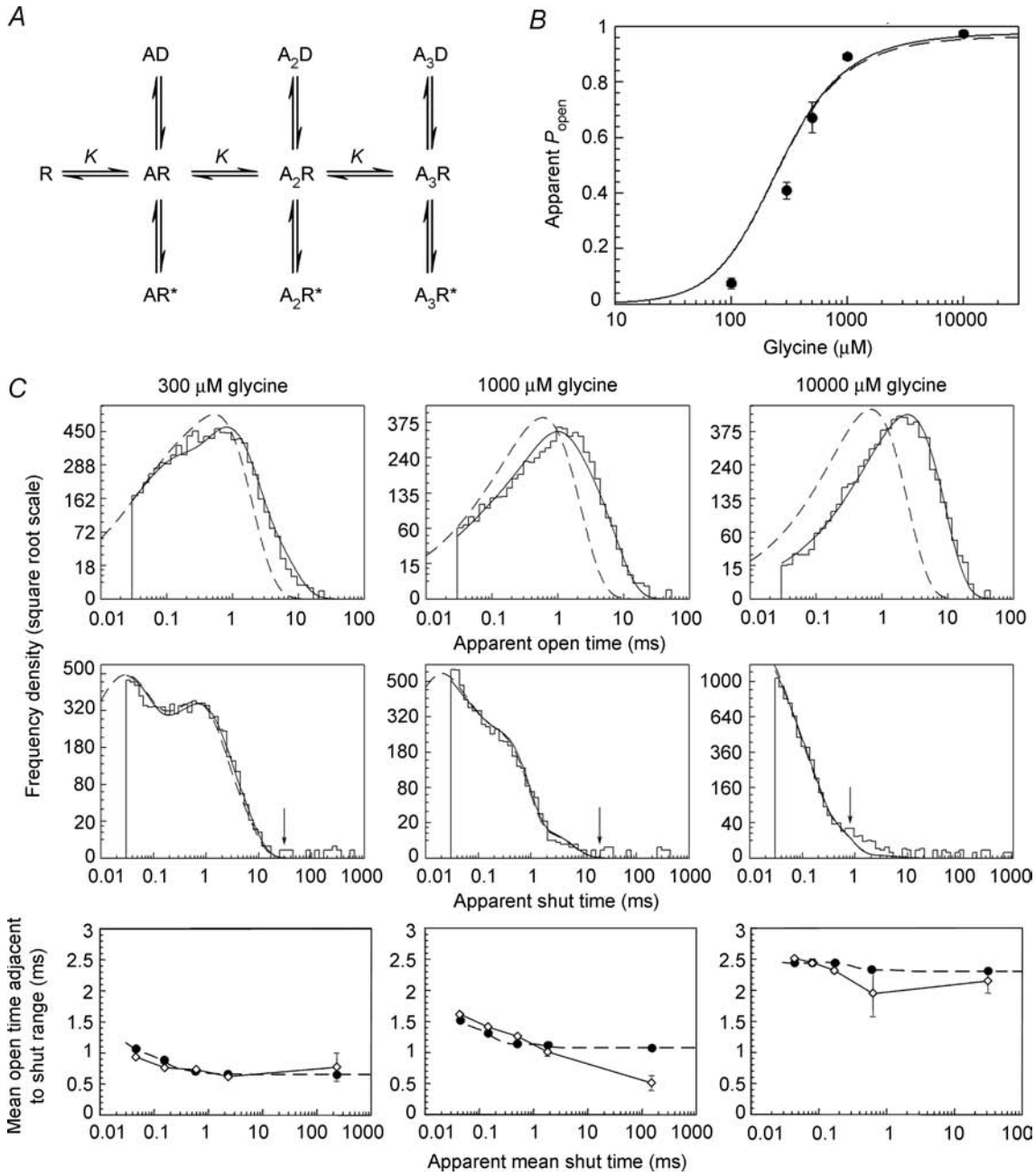

Figure 8. When the binding of glycine is allowed to vary with the level of liganding, the description of the data for the αA52S mutant is slightly improved
This mechanism (*A*, Scheme 2 of Fig. 5) had 18 free parameters. On average, the P_{open}–concentration response data (*B*) were better predicted by the steeper curve that this mechanism produced, than when the binding affinities were constrained to be the same for each step. There was no noticeable improvement in the description of dwell times or correlation plots (*C*), which were fitted very well. Only shut times shorter than t_{crit} (arrow) were used for fitting (see legend to Fig. 6).

Table 5. Fit to α1A52S heteromeric glycine receptor data of the Jones and Westbrook model with interaction between the binding sites (Scheme 2 of Figs 5 and 8), rate and equilibrium constant estimates

	Unit	Mean estimates	Coefficient of variation (%)	Mean estimates for wild-type $\alpha1\beta$
α_1	s^{-1}	9100	3	3400
β_1	s^{-1}	1500	10	400
α_2	s^{-1}	2000	5	2200
β_2	s^{-1}	27000	8	28000
α_3	s^{-1}	1600	17	3700
β_3	s^{-1}	65000	13	112000
d_{-1}	s^{-1}	300	11	1100
d_{+1}	s^{-1}	200	24	20000
d_{-2}	s^{-1}	4900	9	7400
d_{+2}	s^{-1}	3400	12	15000
d_{-3}	s^{-1}	14000	16	17600
d_{+3}	s^{-1}	7300	12	2000
k_{-1}	s^{-1}	3300	11	4000
k_{+1}	$M^{-1}\,s^{-1}$	2.4×10^6	4	0.35×10^6
k_{-2}	s^{-1}	9700	16	2080
k_{+2}	$M^{-1}\,s^{-1}$	4.8×10^6	19	30×10^6
k_{-3}	s^{-1}	1800	46	1700
k_{+3}	$M^{-1}\,s^{-1}$	3.7×10^6	61	160×10^6
E_1	—	0.2	11	0.1
E_2	—	13	3	12.7
E_3	—	41	6	30
D_1	—	0.7	26	10
D_2	—	0.7	20	2.1
D_3	—	0.6	20	0.116
K_1	μM	1400	16	14000
K_2	μM	2100	12	200
K_3	μM	620	16	10
EC_{50}	μM	310	6	67
n_H	—	1.68	5	2.58

The figures are averages of fits to four data sets (see Methods). Values for wild-type $\alpha1\beta$ receptors are from fits of the same model in Burzomato *et al.* (2004).

This led Burzomato *et al.* (2004) to postulate the flip mechanism in which an extra shut state is interposed between the resting state and the open state (Scheme 3 in Figs 5 and 9). In other words, it is postulated that a conformation change (to the flipped conformation) occurs after binding but before opening. If the channel spends enough time in the flipped states, their existence should be detectable, and measurable, in single-channel recordings. This approach has the enormous advantage that there is no longer any need to suppose that distant binding sites interact. Rather than saying, for the wild-type heteromer, that the affinity for binding increases 65-fold for each molecule that is bound, all one has to postulate is that the affinity for binding to the flipped conformation is 65-fold greater than for binding to the resting conformation (Burzomato *et al.* 2004). But for any particular conformation of the receptor, the binding sites are independent, so the binding affinity does not depend on whether other sites are occupied or not.

The fit of the flip model to observations with the αA52S mutant heteromer is shown in Fig. 9, and the values for the rate constants are given in Table 6.

The flip mechanism describes the data well. It is found (Table 6) that the affinity of the flipped conformation for glycine is only about twice that for the resting conformation (compared with 65-fold greater for the wild-type heteromer; Burzomato *et al.* 2004). This result is what would be expected, given the greatly reduced 'binding cooperativity' seen when fitting the Jones–Westbrook-type model.

Some of the rate constants for the flip model were found to be rather variable from one set of experiments to another. Particularly, the rate constants for transitions between resting and flipped conformations were variable (although they were usually quite well defined in each fit). However, the equilibrium constants (as opposed to rate constants) for binding were reasonably consistent (see Table 6).

In the context of the flip model, the agonist efficacy depends on both the equilibrium constant for flipping (F) and the equilibrium constant for the shut–open step (gating; E). The maximum response (P_{open}) depends on both of them, being given by:

$$P_{open}^{max} = \frac{F_3 E_3}{1 + F_3(1 + E_3)} \quad (2)$$

In the wild-type receptor, efficacy increases with the number of ligand molecules bound because both F and E increase, the former effect being the larger (Burzomato *et al.* 2004). In the αA52S mutant heteromer this increase in efficacy as more molecules are bound is largely a result of increases in the gating constants (E). The gating constant for the fully liganded mutant receptor, and its predicted

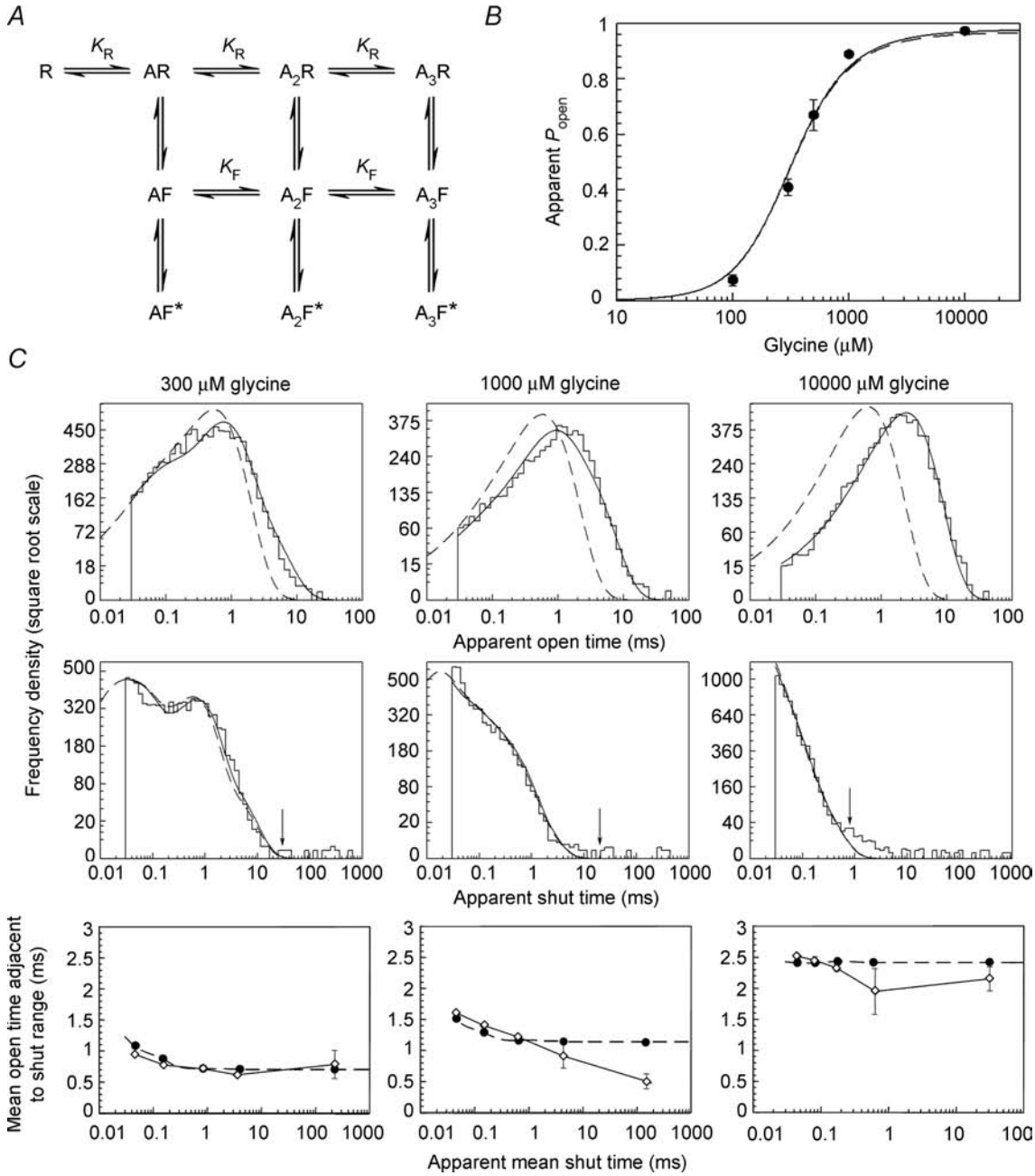

Figure 9. The flip mechanism describes the observed data for αA52S well on all the criteria
The flip mechanism (*A*, Scheme 3 of Fig. 5) has only 14 free parameters, yet predicts the observed P_{open}–concentration relation (*B*) very well. Although the dwell-time distributions (*C*) were not perfectly predicted by the fitted rates, the errors were quite minor and tended to be in the fastest shut times, of which many are missed. Only shut times shorter than t_{crit} (arrow) are used for fitting (see Fig. 6 legend).

Table 6. Fit to α1A52S heteromeric glycine receptor data of the flip model (Scheme 3 of Figs 5 and 9), rate and equilibrium constant estimates

	Unit	Mean estimates	Coefficient of variation (%)	Mean estimates for wild-type $\alpha1\beta$
α_1	s^{-1}	12800	7	3400
β_1	s^{-1}	3400	62	4200
α_2	s^{-1}	2200	7	2100
β_2	s^{-1}	17500	25	28000
α_3	s^{-1}	1400	8	7000
β_3	s^{-1}	61000	7	129000
γ_1	s^{-1}	108000	50	29000
δ_1	s^{-1}	77000	81	180
γ_2	s^{-1}	7400	60	18000
δ_2	s^{-1}	6700	32	6800
γ_3	s^{-1}	5200	27	900
δ_3	s^{-1}	13000	9	20900
k_-	s^{-1}	1300	38	300
k_+	$M^{-1}\,s^{-1}$	0.8×10^6	30	0.59×10^6
k_{F-}	s^{-1}	6800	37	1200
k_{F+}	$M^{-1}\,s^{-1}$	16×10^6	74	150×10^6
E_1	—	0.3	63	1.3
E_2	—	8	18	13
E_3	—	45	6	20
F_1	—	1.1	60	6×10^{-3}
F_2	—	1.6	27	0.40
F_3	—	3.0	17	27
K_R	μM	1600	16	520
K_F	μM	840	24	8
EC_{50}	μM	310	7	68
n_H	—	1.7	8	2.44

The figures are averages of fits to four data sets (see Methods). Values for wild-type $\alpha1\beta$ receptors are from fits of the same model in Burzomato *et al.* (2004).

maximum P_{open}, are both at least as large as for the wild-type heteromer.

Constrained fits with the flip mechanism. In the flip model (Fig. 9), the open states are not connected. In other words, it has been assumed that dissociation from the open channel is slow enough that it has little effect on the observations. If the open states are connected, there is no increase at all in the number of free parameters if we suppose that the binding sites on the open conformation are independent (as already assumed for the two shut conformations), and that the new cycles that are introduced obey microscopic reversibility. Given these assumptions, adding two links between the open states gives a model that is more constrained than that in Fig. 9, not less constrained as might at first sight be expected. In particular, the values of E are constrained to increase by the same factor for each extra glycine molecule that is bound. This factor is not constant in the fit given in Table 6, so it is perhaps not surprising that fits done with the open states connected (data not shown) were less good than those shown in Fig. 9.

Because the A52S mutation is not in the binding site, it might be expected that the mutation would not alter the resting-state affinity for the agonist. We tested this hypothesis by fitting the flip model with the microscopic glycine association and dissociation rates in the resting state constrained in two ways. Firstly, we fixed the association and dissociation rates to the mean values that were determined for wild-type receptors by Burzomato *et al.* (2004) ($k_+ = 0.59 \times 10^6\ M^{-1}\,s^{-1}$ and $k_- = 300\ s^{-1}$). The flip mechanism with these additional constraints has 12 free parameters. The description of the observed dwell times and conditional distributions that we obtained from the estimated rates was very poor, and the P_{open}–concentration curve was too shallow (data not shown). In order to relax this constraint slightly, in another fit the binding of glycine to the resting state was constrained to have the same equilibrium constant as for wild-type receptors (520 μM). This allowed one more free parameter (total 13), but the fits were not improved. It appears that the observed data for the mutant receptor are

incompatible with a resting affinity that is the same as that for the wild-type receptor.

Discussion

We have studied a naturally occurring murine mutation in recombinant glycine receptors. Mice that are homozygotes for the *spasmodic* mutation carry the mutation in both glycine receptor α1 subunit alleles, and are susceptible to brief startle attacks, like humans with the rare disease hyperekplexia. Presumably this is a result of reduced glycinergic inhibition in the spinal cord.

This is the first loss-of-function mutation that has been studied with the HJCFIT method, and the first mutation in the glycine receptor that has been studied in detail at the single-channel level.

Our work was carried out in a recombinant system, but we have good reason to believe that heteromeric glycine receptors as expressed in HEK cells are similar to those in central synapses (Beato & Sivilotti, 2007). As the mutation is recessive, it is likely that all the α subunits expressed by a cell (and hence in a synapse) harbour the mutation, in mice with the *spasmodic* phenotype.

What is the effect of the mutation?

In order to draw conclusions about the physical nature of the process of activation by glycine, and of the effects of a mutation on that process, we must postulate a reaction mechanism that describes physical reality. It is not possible to make inferences about the physical effects of a mutation in a way that is 'model-free'. The most plausible mechanism that we have for the glycine receptor is the flip model (Scheme 3, Fig. 5), and our conclusions will be based on that.

Our analysis of the αA52S mutation had some limitations, largely as a result of the fact that we could not include low-concentration results in the analysis. At high concentrations it was possible to select records that showed homogenous behaviour, but at low concentrations this was not possible. In addition, the fact that the mutation shortens open-time durations means that more brief events are missed than for wild-type receptors, thus limiting resolution.

However, it is equally true that glycine receptors offer advantages in experimental design that other receptors do not. Glycine molecules act only as agonists, and do not block the channel of the glycine receptor, meaning that activations can be equally well detected at any concentration, no matter how high. This was critically important given that we chose to study a loss-of-function mutation. The same is not true for nicotinic receptors, where agonists also tend to block the channel pore. This fast block progressively reduces the apparent amplitude of activations with increasing concentration, leading to problems in measuring P_{open} clusters at high concentrations, even in wild-type receptors (Ogden & Colquhoun, 1985, Colquhoun and Ogden, 1988).

We did not manage to obtain good descriptions of the data with mechanisms that had fewer than three binding sites. Therefore the present work on the αA52S mutant confirms our earlier finding in wild-type receptors (both homomeric and heteromeric), that glycine receptors are well described by mechanisms that include three binding sites (Beato *et al.* 2004; Burzomato *et al.* 2004). Which subunits form these binding sites, and how they are arranged is beyond the scope of this work and is unimportant for our conclusions. It should however, be noted that, in common with wild-type receptors, we could only obtain good descriptions of the data with mechanisms that allowed binding sites to interact. Mechanisms that assumed that the binding sites were initially different but did not allow them to interact did not provide a good fit.

All activation mechanisms that fit wild-type heteromeric receptors include a strong increase in the *apparent* affinity of glycine binding as more binding sites become occupied by agonist. The binding to the resting state appears relatively weak, but as successive glycine molecules bind, the binding appears to become increasingly tight. In the A52S mutant heteromeric receptor, this apparent 'cooperativity' of glycine binding is almost entirely absent, a qualitative conclusion that is not strongly dependent on the details of the mechanism insofar as it is seen in both the Jones and Westbrook-type mechanism (Table 5, Fig. 8) and the flip mechanism (Table 6, Fig. 9).

A second conclusion that does not depend to any great extent on the mechanism fitted is that there is only a limited effect of the mutation on the gating of the receptor. By gating, we mean the final step in the opening of the pore which allows ions to flow through the channel, and the first event at the end of an opening of the pore that terminates this flow. The maximum P_{open} that could be attained at high agonist concentrations was similar for wild-type and mutant. For the mutant receptors, the gating equilibrium constant for the fully liganded channel was $E_3 = 41$ for the Jones–Westbrook-type mechanism (Table 5, maximum $P_{open} = E_3/(1 + E_3 + D_3) = 0.96$), or for the flip model $E_3 = 45$, $F_3 = 3.0$ (Table 6, maximum $P_{open} = E_3F_3/(1 + F_3 + E_3F_3) = 0.97$). This is as efficient as wild-type gating, which gave Burzomato *et al.* (2004) for the Jones–Westbrook-type mechanism, $E_3 = 30$, maximum $P_{open} = 0.97$, and for the flip mechanism, $E_3 = 20$, $F_3 = 27$, maximum $P_{open} = 0.95$. The brief shut times that we observed in the αA52S mutant receptor (mean lifetime 13–23 μs, Table 2) were also similar to those observed in the wild-type heteromeric receptor, mean lifetime 12–15 μs (Burzomato *et al.* 2004), which

shows that the behaviour of wild-type and mutant receptors is similar when they are saturated with agonist.

What differs between the rival mechanisms is the physical interpretation that is placed on the observed 'reduction of cooperativity' seen in the mutant receptor. In the Jones–Westbrook-type of mechanism, it is implicit that an empty binding site can be influenced by whether or not a different binding site is occupied, despite the fact that they are quite a long way apart. The way in which such an influence might be propagated is not specified in the mechanism. The extra shut states (D states in Scheme 2, Fig. 5) play no part in the 'cooperativity', and there is no independent evidence that they have any physical existence; they are essentially arbitrary states that are needed to get a good fit.

In the flip mechanism, on the other hand, we postulate an extra shut conformation that is intermediate between the resting state and the open state. These extra shut states are part of the transduction pathway, and there is evidence from other approaches that such short-lived intermediates must exist (Chakrapani *et al.* 2004). In the case of the wild-type receptor, the flip approach allows a much simpler physical interpretation (Burzomato *et al.* 2004; Colquhoun & Sivilotti, 2004). Binding to each site is supposed to be quite independent of whether other sites are occupied or not, and the appearance of interaction arises solely from the fact that the affinity of the agonist for the flipped conformation (F in Scheme 3, Fig. 5) is 65 times higher that it is for the resting conformation. The explanation is closely analogous to that first suggested for haemoglobin by Wyman & Allen (1951) and subsequently embodied in Monod *et al.* (1965). In this interpretation, the effect of the αA52S mutation is mainly to reduce the selectivity of glycine for the flipped conformation. The equilibrium constant for flipping of the fully liganded channel (F_3, Table 6) is reduced about nine-fold: this could be produced by an effect of the mutation on any part of the molecule that participates in the conformation change between resting and flipped. Rather than the affinity for glycine being 65-fold greater for the flipped than for the resting conformation as in the wild type, the mutation reduces this selectivity to a factor of less that two-fold. The affinity for the resting state (K_R, Table 6) is itself reduced by a factor of about three, but the affinity for the intermediate flipped conformation (K_F) is reduced by a factor of over 100-fold. The physical nature of the flipping conformation change is not known, but it is not surprising that it can be affected by a mutation, such as αA52S, which is not in the binding site itself. It is tempting to speculate that the physical counterpart of the flipped conformation is the 'domain closure' that is known to take place in the extracellular domain of the receptor upon agonist binding (reviewed in Colquhoun & Sivilotti, 2004; Sine & Engel, 2006).

The effect on the resting affinity is likely to be real because fits that we have done with binding affinities constrained to be the same as in the wild-type receptor gave bad descriptions of the data, and nonsensical values for some rate constants. This change in resting affinity implies that the mutation, though not within the binding site itself, can nevertheless have, indirectly, a modest effect on the resting structure of the binding site.

Predicted effect of the mutation on synaptic currents

Recent work by Graham *et al.* (2006) shows that in homozygous *spasmodic* mice, mIPSCs mediated by glycine on hypoglossal motoneurones *in vitro* decay faster (decay time constant 2.7 ms) than those recorded in control mice (5 ms). Using the flip mechanism with rates as in Table 6, we simulated a synaptic current by calculating the relaxation of A52S receptors in response to a 1 ms pulse of 1 mM glycine, using the program SCALCS, www.ucl.ac.uk/Pharmacology/dc.html. The predominant time constant of the decay for A52S receptors was about twice as fast as that predicted by the flip mechanism as fitted to wild-type heteromeric receptors, and in good agreement with native currents (3 ms for A52S *versus* 6 ms for wild type, wild-type rates from Burzomato *et al.* 2004). Our fitted mechanisms for A52S did not predict smaller peak currents than wild-type. In *spd/spd* mice, mIPSCs were observed to be smaller (as well as faster), but this could arise from reduced receptor number (Graham *et al.* 2006). We note that the A52S mutation has no effect on channel conductance. However, the as-yet undetermined concentration profile of glycine in the synaptic cleft is a critical parameter that determines the size of synaptic currents and the currents that we simulate.

Implications for structure–function relationships in cysteine-loop receptors

Much of the available analysis of cysteine-loop receptor gating at the single-channel level comes from the study of mutations in muscle nicotinic receptors. A working hypothesis for the principal gating pathway leading to the opening of the pore has been proposed (Lee & Sine, 2005), and many naturally occurring disease mutations that severely alter receptor function occur along this pathway. The perturbation produced by binding must be transmitted through the molecule to the channel gate. The critical areas involved in this transduction are thought to include the M2–M3 loop and the region of the receptor at the interface between the membrane helices and the agonist-binding domain, where the A52S mutation is found (Colquhoun & Sivilotti, 2004; Sine & Engel, 2006).

Because of this picture of receptor activation, initially it may appear odd that we do not detect any changes in the

gating of the A52S mutant receptor, and that the binding of agonist molecules is where we observe the greatest changes. One explanation for this apparent discrepancy is that the kind of conformational changes suggested by the flip mechanism propagate not only within subunits, but also between subunits. Such interactions must involve the subunit interfaces, and possibly movement of subunits relative to each other. The mutation seems to reduce the effects of any such conformational change, effectively changing the dissociation constant of the binding sites at a distance. It is not without interest that the binding sites, whose affinity for glycine is increased following the conformational change in wild-type receptors, are located within subunit interfaces.

We have not yet reached the stage where it is possible to make accurate predictions of the effects on function of changes in structure. There are several examples of mutations in nicotinic receptors that appear to have paradoxical effects on ligand binding, despite being located well outside the binding site. These include α1N217K (Wang *et al.* 1997) and ϵL221F (Hatton *et al.* 2003), both of which are in or near the first transmembrane domain, as well as α1G153S (Sine *et al.* 1995). It is possible that the effects observed in these cases are due to as-yet unexplained biases in our analyses, and this may be true for glycine receptors too.

In the absence of glycine receptor structural information, we must relate our functional data to the structure of the homologous snail acetylcholine-binding protein (Brejc *et al.* 2001). Recent refinements of these structures in *apo* and agonist-bound conformations show that agonist binding promotes a large translation of the C-loop and a small outward movement of loop F (Hansen *et al.* 2005). Loop F is adjacent to the A52S mutation in glycine receptors, at the base of the extracellular domain, and folds toward the neighbouring subunit in the *Aplysia*–Ach-binding protein (AChBP) structure (Fig. 10). Residues in close proximity to the site of the A52S mutation participate in a network of solvent-mediated intermolecular hydrogen bonds between loops 2 and F. The composition of loop F varies across the superfamily, but a conserved feature is that it ends with an aromatic residue. In *Aplysia*–AChBP, a tyrosine makes a water-mediated hydrogen bond (*via* W2, see Fig. 10) to the carbonyl oxygen at the tip of loop 2. This part of the interfacial region (and probably others) could be responsible for propagating the conformational changes that correspond to the flipped state of the channel between subunits, which could be disrupted by the A52S mutation. It is equally possible that the A52S mutation reduces the affinity of the binding site for agonist by hindering translation of loop C within the same subunit. Clearly, more studies of residues that lie at the interfaces between subunits are required to understand the role of these interactions in cysteine-loop receptor gating.

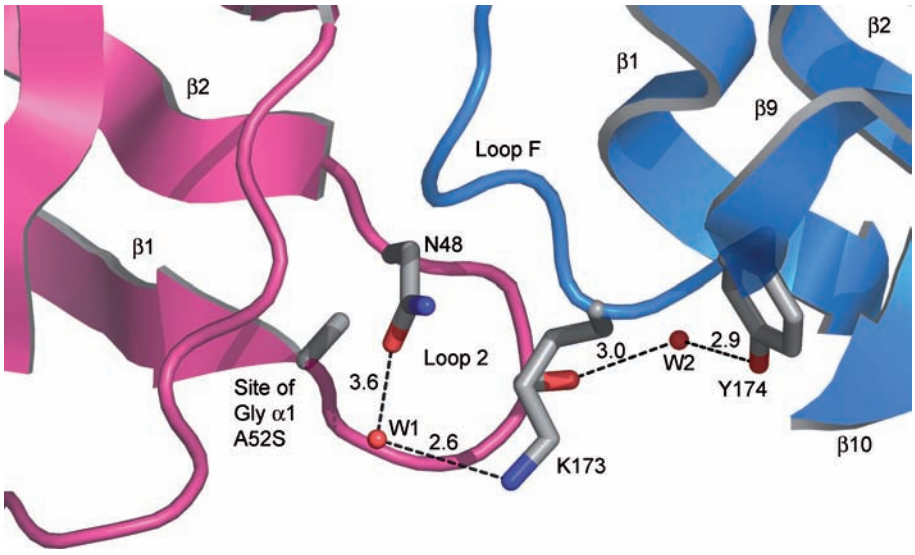

Figure 10. Close-up of the subunit interface at the base of the apo *Aplysia*-AChBP crystal structure
This region would be immediately above the membrane domains, which begin after the β10 strand, in the full-length receptor. Two out of the five protomers are shown (B in pink and C in blue). The probable position of the A52S mutation is marked, as an alanine, in protomer B. The adjacent intersubunit hydrogen bond network between loops 2 and F is shown as dotted lines, with water molecules in red (W1 and W2). Residues are numbered according to the *Aplysia* AChBP sequence. According to published structure-based sequence alignments (Brejc *et al.* 2001; Hansen *etal.* 2004), the correspondence between residues is as follows: Asn48 in *Aplysia*-AChBP is Met in the glycine receptor α1 subunit, Lys173 is Gln and Tyr174 is Phe. The bulky aromatic residue at the beginning of the β9 strand is conserved across the superfamily. Bond lengths are in Angstroms.

References

Bakker MJ, Van Dijk JG, van den Maagdenberg AM & Tijssen MA (2006). Startle syndromes. *Lancet Neurol* **5**, 513–524.

Beato M, Groot-Kormelink PJ, Colquhoun D & Sivilotti LG (2002). Openings of the rat recombinant $\alpha 1$ homomeric glycine receptor as a function of the number of agonist molecules bound. *J Gen Physiol* **119**, 443–466.

Beato M, Groot-Kormelink PJ, Colquhoun D & Sivilotti LG (2004). The activation of $\alpha 1$ homomeric glycine receptors. *J Neuroscience* **24**, 895–906.

Beato M & Sivilotti LG (2007). Single-channels properties of glycine receptors of juvenile rat spinal motoneurones *in vitro*. *J. Physiol* (in press, DOI 10.1113/jphysiol.2006.125740).

Benndorf K (1995). Low-Noise Recording. In *Single-Channel Recording*, ed. Sakmann B & Neher E, pp. 129–153. Plenum Press, New York.

Bormann J, Hamill OP & Sakmann B (1987). Mechanism of anion permeation through channels gated by glycine and γ-aminobutyric acid in mouse cultured spinal neurones. *J Physiol* **385**, 243–286.

Brejc K, van Dijk WJ, Klaassen RV, Schuurmans M, van der Oost J, Smit AB & Sixma TK (2001). Crystal structure of an ACh-binding protein reveals the ligand-binding domain of nicotinic receptors. *Nature* **411**, 269–276.

Burzomato V (2005). The activation mechanism of the $\alpha 1\beta$ heteromeric glycine receptor. *PhD Thesis* University of London.

Burzomato V, Beato M, Groot-Kormelink PJ, Colquhoun D & Sivilotti LG (2004). Single-channel behavior of heteromeric $\alpha 1\beta$ glycine receptors: an attempt to detect a conformational change before the channel opens. *J Neurosci* **24**, 10924–10940.

Burzomato V, Groot-Kormelink PJ, Sivilotti LG & Beato M (2003). Stoichiometry of recombinant heteromeric glycine receptors revealed by a pore-lining region point mutation. *Receptors Channels* **9**, 353–361.

Chakrapani S, Bailey TD & Auerbach A (2004). Gating dynamics of the acetylcholine receptor extracellular domain. *J Gen Physiol* **123**, 341–356.

Colquhoun D (1998). Binding, gating, affinity and efficacy: The interpretation of structure-activity relationships for agonists and of the effects of mutating receptors. *Br J Pharmacol* **125**, 923–947.

Colquhoun D, Hatton CJ & Hawkes AG (2003). The quality of maximum likelihood estimates of ion channel rate constants. *J Physiol* **547**, 699–728.

Colquhoun D, Hawkes AG & Srodzinski K (1996). Joint distributions of apparent open and shut times of single-ion channels and maximum likelihood fitting of mechanisms. *Phil Trans R Soc Lond A* **354**, 2555–2590.

Colquhoun D & Ogden DC (1988). Activation of ion channels in the frog end-plate by high concentrations of acetylcholine. *J Physiol* **395**, 131–159.

Colquhoun D & Sigworth FJ (1995). Fitting and statistical analysis of single-channel records. In *Single-Channel Recording*, ed. Sakmann B & Neher E, pp. 483–587. Plenum Press, New York.

Colquhoun D & Sivilotti LG (2004). Function and structure in glycine receptors and some of their relatives. *Trends Neurosci* **27**, 337–344.

Gill SB, Veruki ML & Hartveit E (2006). Functional properties of spontaneous IPSCs and glycine receptors in rod amacrine (AII) cells in the rat retina. *J Physiol* **575**, 739–759.

Graham BA, Schofield PR, Sah P, Margrie TW & Callister RJ (2006). Distinct physiological mechanisms underlie altered glycinergic synaptic transmission in the murine mutants *spastic*, *spasmodic*, and *oscillator*. *J Neurosci* **26**, 4880–4890.

Groot-Kormelink PJ, Beato M, Finotti C, Harvey RJ & Sivilotti LG (2002). Achieving optimal expression for single channel recording: a plasmid ratio approach to the expression of $\alpha 1$ glycine receptors in HEK293 cells. *J Neurosci Methods* **113**, 207–214.

Grosman C, Zhou M & Auerbach A (2000). Mapping the conformational wave of acetylcholine receptor channel gating. *Nature* **403**, 773–776.

Grudzinska J, Schemm R, Haeger S, Nicke A, Schmalzing G, Betz H & Laube B (2005). The β subunit determines the ligand binding properties of synaptic glycine receptors. *Neuron* **45**, 727–739.

Hansen SB, Sulzenbacher G, Huxford T, Marchot P, Taylor P & Bourne Y (2005). Structures of Aplysia AChBP complexes with nicotinic agonists and antagonists reveal distinctive binding interfaces and conformations. *EMBO J* **24**, 3635–3646.

Hansen SB, Talley TT, Radic Z & Taylor P (2004). Structural and ligand recognition characteristics of an acetylcholine-binding protein from *Aplysia californica*. *J Biol Chem* **279**, 24197–24202.

Hatton CJ, Shelley C, Brydson M, Beeson D & Colquhoun D (2003). Properties of the human muscle nicotinic receptor, and of the slow-channel myasthenic syndrome mutant ϵL221F, inferred from maximum likelihood fits. *J Physiol* **547**, 729–760.

Hawkes AG, Jalali A & Colquhoun D (1990). The distributions of the apparent open times and shut times in a single channel record when brief events can not be detected. *Philos Trans R Soc Lond A* **332**, 511–538.

Hawkes AG, Jalali A & Colquhoun D (1992). Asymptotic distributions of apparent open times and shut times in a single channel record allowing for the omission of brief events. *Philos Trans R Soc Lond B* **337**, 383–404.

Jones MV & Westbrook GL (1995). Desensitized states prolong $GABA_A$ channel responses to brief agonist pulses. *Neuron* **15**, 181–191.

Lane PW, Ganser AL, Kerner AL & White WF (1987). Spasmodic, a mutation on chromosome 11 in the mouse. *J Hered* **78**, 353–356.

Lee WY & Sine SM (2005). Principal pathway coupling agonist binding to channel gating in nicotinic receptors. *Nature* **438**, 243–247.

Lester HA, Dibas MI, Dahan DS, Leite JF & Dougherty DA (2004). Cys-loop receptors: new twists and turns. *Trends Neurosci* **27**, 329–336.

Lynch JW (2004). Molecular structure and function of the glycine receptor chloride channel. *Physiol Rev* **84**, 1051–1095.

Mascia MP, Mihic SJ, Valenzuela CF, Schofield PR & Harris RA (1996). A single amino acid determines differences in ethanol actions on strychnine-sensitive glycine receptors. *Mol Pharmacol* **50**, 402–406.

Miller PS, da Silva HM & Smart TG (2005). Molecular basis for zinc potentiation at strychnine-sensitive glycine receptors. *J Biol Chem* **280**, 37877–37884.

Monod J, Wyman J & Changeux J-P (1965). On the nature of allosteric transitions: a plausible model. *J Mol Biol* **12**, 88–118.

Ogden DC & Colquhoun D (1985). Ion channel block by acetylcholine, carbachol and suberyldicholine at the frog neuromuscular junction. *Proc R Soc Lond B Biol Sci* **225**, 329–355.

Praveen V, Patole SK & Whitehall JS (2001). Hyperekplexia in neonates. *Postgraduate Med J* **77**, 570–572.

Ryan SG, Buckwalter MS, Lynch JW, Handford CA, Segura L, Shiang R, Wasmuth JJ, Camper SA, Schofield P & O'Connell P (1994). A missense mutation in the gene encoding the α1 subunit of the inhibitory glycine receptor in the spasmodic mouse. *Nature Genet* **7**, 131–135.

Sakmann B, Patlak J & Neher E (1980). Single acetylcholine-activated channels show burst-kinetics in presence of desensitizing concentrations of agonist. *Nature* **286**, 71–73.

Saul B, Schmieden V, Kling C, Mulhardt C, Gass P, Kuhse J & Becker C-M (1994). Point mutation of glycine receptor α1 subunit in the spasmodic mouse affects agonist responses. *FEBS Lett* **350**, 71–76.

Sine SM & Engel AG (2006). Recent advances in Cys-loop receptor structure and function. *Nature* **440**, 448–455.

Sine SM, Ohno K, Bouzat C, Auerbach A, Milone M, Pruitt JN & Engel AG (1995). Mutation of the acetylcholine receptor α subunit causes a slow-channel myasthenic syndrome by enhancing agonist binding affinity. *Neuron* **15**, 229–239.

Unwin N (2005). Refined structure of the nicotinic acetylcholine receptor at 4 Å resolution. *J Mol Biol* **346**, 967–989.

Wang H-L, Auerbach A, Bren N, Ohno K, Engel AG & Sine SM (1997). Mutation in the M1 domain of the acetylcholine receptor α subunit decreases the rate of agonist dissociation. *J Gen Physiol* **109**, 757–766.

Wilkins ME & Smart TG (2002). Redox modulation of $GABA_A$ receptors obscured by Zn^{2+} complexation. *Neuropharmacology* **43**, 938–944.

Wyman J & Allen DW (1951). The problem of the heme Interactions in hemoglobin and the basis of the Bohr effect. *J Polymer Sci* **VII**, 499–518.

Acknowledgements

This work was funded by the MRC (Grant G0400869 to L.G.S. and D.C.) and the Wellcome Trust (grant 064652 to L.G.S). We thank Drs M. Beato, V. Burzomato and R. Lape for helpful discussions and help with data analysis.

Authors' present addresses

A. J. R. Plested: LCMN, NICHD, NIH Building 35, 35 Convent Drive, Bethesda, MD, USA.

P. J. Groot-Kormelink: Novartis Horsham Research Centre, Wimblehurst Road, Horsham RH12 5AB, UK.